Development of a Non-Instrumented Point-of-Care (POC) HIV-1 Diagnostic Device

Nuvala T. Fomban

A thesis submitted in partial fulfillment of the requirements for the degree of

Master of Science in Bioengineering

University of Washington

2013

Program Authorized to offer Degree:
Bioengineering

University of Washington
Abstract

Development of a Non-Instrumented Point-of-Care (POC) HIV-1 Diagnostic Device

Nuvala T. Fomban

Chair of the Supervisory Committee
Professor Patrick S. Stayton
Department of Bioengineering

There is a growing need for sensitive, simple, affordable and rapid detection of infectious disease biomarkers for faster access to test results and improved patient outcomes. The development of rapid, portable and accurate POC clinical diagnostic devices could lower transmission rates, especially in cases of recent HIV infection in Resource Limited Settings (RLS) by providing timely access to intervention. Self-powered assays will be affordable, dependable and efficient for RLS with minimal user training. The clinical impact of HIV rapid testing technologies in patient care will be to achieve earlier, faster infection identification, allowing immediate counseling and treatment using Antiretrovirals (ARVs).

In this thesis, we developed an inexpensive and rapid diagnostics module for the capture and enrichment of an analyte from pooled human plasma samples. We have developed a flow-through membrane based system combining covalently conjugated polymer-antibodies and detection conjugates in a simultaneous binding, capture, and detection assay with potential adaptation for low-resource settings. This flow-through assay module provides immunocomplex capture and detection of HIV-1 p24 antigen on a porous membrane surface for visualization and semi-quantification. We investigated two formats of rapid immunocomplex capture where the visual signal is developed after surface capture

of an enzyme detection sandwich and addition of precipitating substrate, and the second, where a signal was directly visualized with gold colloid nanoparticles (AuNPs). This former system was optimized to provide two-step immunocomplex capture and detection for application to HIV-1 p24 antigen using a prototype disc device. Using this flow-through system, we detected 10pg/ml of p24 antigen in 50% human plasma as positive signal above background, reproducible with a coefficient of variation of <10%. Finally, the later membrane p24 assay system was optimized to enrich picomolar concentrations of HIV-1 p24 antigen in milliliter volume samples using a non-instrumented self-powered prototype syringe device with gold nanoparticles as the detection system. The final assay system has been adapted for RLSs using a non-instrumented device with heat generation capabilities. In this self-powered heating device, we use the exothermic reaction of sodium acetate trihydrate and water to generate heat. The development of the prototype non-instrumented flow-through immunoassay-heating device represents the first example of using an exothermic chemical reaction to generate the heat needed for thermally mediated immunoassays in building a fully functional and electricity-free diagnostic device for HIV. Using this flow-through system with incorporated device, we detected 12.5pg/ml of p24 antigen in 20% human plasma as positive signal above background, reproducible with a coefficient of variation of <15%. This thesis presents an initial prototype non-instrumented flow-through immunoassay device for HIV p24 antigen capable of detecting picogram per milliliter from milliliter plasma samples yielding results in less than 30 minutes.

TABLE OF CONTENTS

LIST OF FIGURES

LIST OF TABLES

ACKNOWLEDGMENTS

The author wishes to express sincere appreciation to the Department of Bioengineering at the University of Washington and particularly Professor Patrick Stayton for his continuous patience, devotion, advice, support and guidance over the years. The author is also very thankful to Professor James Lai for his advice and support in completing this project. He is very grateful to the past and present staff and members of the Stayton group for their help, countless feedback, support, and encouragements. Some parts of this project would have never been possible without funding provided by the Life Science Discovery Fund (Grant # 2376827) and the collaboration of The Program for Appropriate Technology in Health (PATH) team led by Dr. Gonzalo Domingo and Dr. Bernhard H. Weigl. Special acknowledgements go to Jeremy Capalungan for initial antibody screening and Paul LaBarre, Jered Singleton and Shawn McGuire for device development. I am very thankful to my friends and family for their encouragement and support.

Chapter 1

Motivation, Significance and Background

1.1 Motivation for Rapid HIV Point-of-Care (POC) Testing

In 2008, the CDC reported that there are approximately 56,000 new HIV infections each year with more Americans living with HIV than ever before. In 2010, the majority of the world's 34 million HIV-infected patients lived in resource-limited settings (RLS) of sub-Saharan Africa, Asia, and S. America where sensitive diagnostic POC technologies are

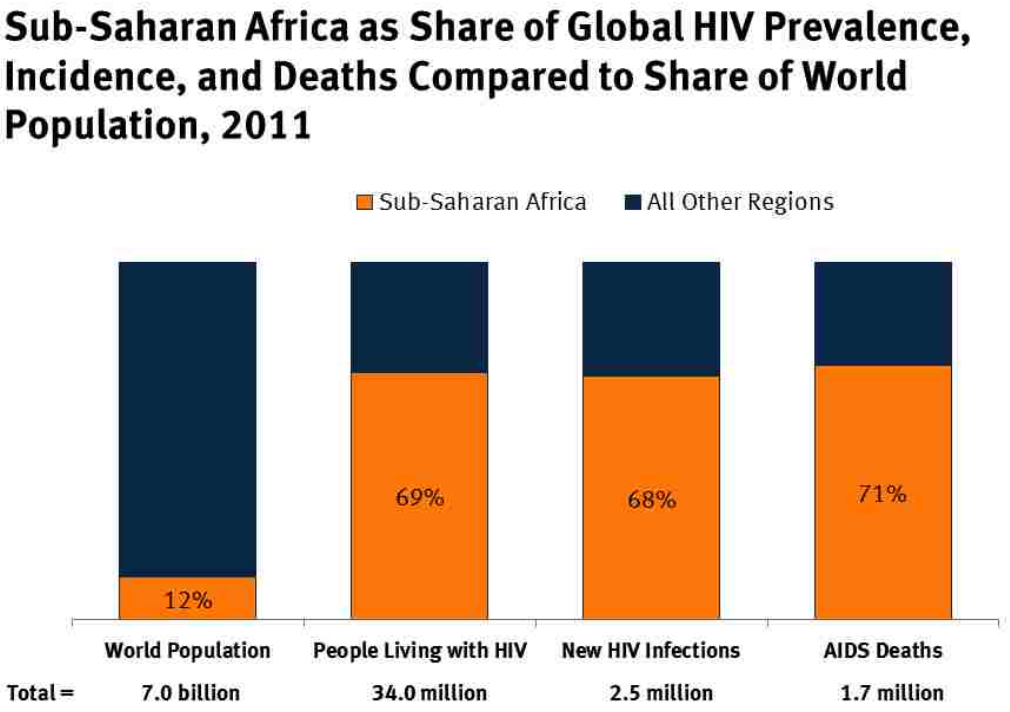

Figure 1. HIV demographic and relationship to low resources settings such as sub-Saharan Africa. (Adapted and modified from Kaiser Family Foundation. Data is based on UNAIDS, Report on the Global AIDS Epidemic; 2012 and Population Reference Bureau, 2011 World Population Data Sheet).

absent[8]. Approximately 1.1 million Americans are among the 34 million people living with HIV and almost 25% are age 50 and older[9]. In 2011, an estimated 2.5 million people became infected with HIV, 1.7 million died of AIDS and 7000 are infected[10] every day **(Figure 1).**

HIV rapid testing is critical to prevent unknowing transmission[11]. The principal methods for diagnosing primary HIV infection include detection of viral nucleic acids, viral antibodies (reactive to HIV antigens gp120/160 plus either gp41 or p24), viral p24 antigen, or culturing HIV[12, 13]. During HIV infectious viremia, concentrations of detectable biomarkers in blood vary with time as the disease progresses: RNA>p24 antigen> antibodies> proviral DNA **(Figure 2).** Depending on the route of HIV infection, the

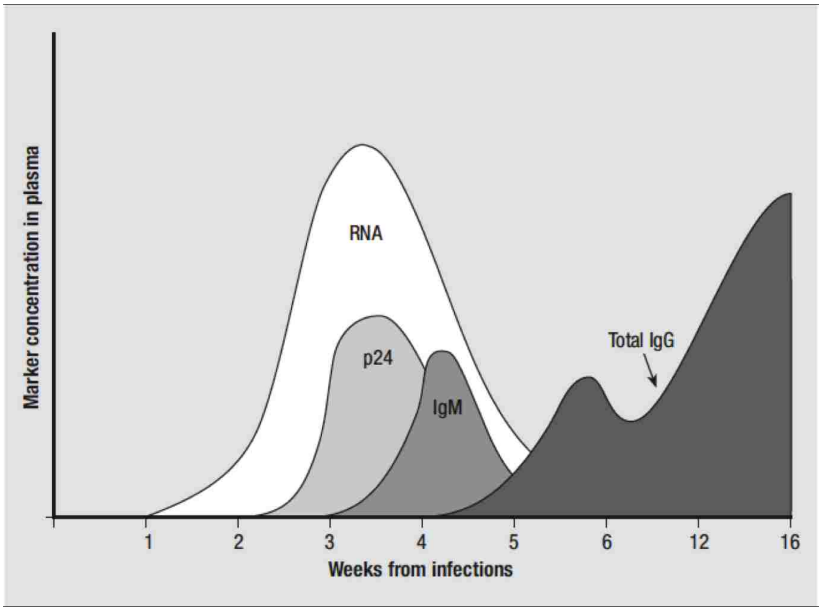

Figure 2. Representation of viral biomarkers during HIV Viremia during the first few weeks of infection with HIV-1[2]. The peak for proviral DNA will be similar to the RNA peak.

Data and details were adapted and modified from Stefano Buttò et al[2] using data from reports by Murphy G. and Parry J.V. and published on EuroSurveillance.org in July 2008 (Vol. 13, Issues 7-9).

presence of HIV-1 RNA in plasma and antibody seroconversion varies between 27.4 and 10.2 days, called the window period (WP) and seroconversion may take six months. HIV seroconversion is part of an immune response that occurs when a person infected with a HIV virus develops antibodies against HIV. A "seroconvert" HIV patient will have HIV antibodies in their blood, will test positive for HIV antibody tests and is at high risk for HIV transmission[14-15].

The WP leads to delayed diagnosis, treatment and disease management. P24 antigen tests detect HIV infection from 9.4 to 17.4 days earlier than most current assays[12, 16], about 6 days before antibody tests become positive, making p24 antigen a replaceable biomarker for early HIV diagnostics. Current challenges for HIV testing include lowering cost, equipment and labor requirements for skilled personnel, and detecting infection earlier. Variation in HIV subtypes (M, N, O and P) can affect test performance. In RLSs, "gold standard" HIV testing, using nucleic acid amplification test (NAAT) and enzyme immunoassay (EIA), is limited to centralized labs. In developed and developing countries, rapid HIV antibody immunochromatographic ("dip-stick") assays represent a major advancement in HIV screening[17]. However, rapid tests are possible only after seroconversion, because HIV-1/2 antibodies only appear in the serum at significant levels 20 to 45 days post infection. Additionally, "dip-stick" assays are limited in sensitivity due to smaller sample volumes (Table 3). There is an unmet need for sensitive, rapid and affordable HIV-1 diagnosis in RLSs. In this work, we have developed a prototype POC HIV diagnostic device using p24 antigen as a target biomarker. This diagnostic device is inexpensive and rapid for the simultaneous capture, enrichment and detection of p24

antigen from human plasma specimens across a flow-through membrane based system with potential adaptation for low-resource settings

1.2 Current State of the Art for Rapid HIV Testing

HIV testing has evolved through 4 generations. The first generation available in 1985 was based on whole viral lysate and used an indirect immunoassay. The second generation tests used synthetic and recombinant peptide antigens, leading to improved sensitivity and specificity[18]. The third generation assays employed sandwich immunoassay formats to detect IgG and IgM antibodies simultaneously. Most clinical labs now use fourth generation assays to detect both antigens and antibodies (Combo diagnostic test) from different patient specimens. Sample type varies based on assay type and format (*e.g.,* serum plasma, dried blood spots, oral fluids or urine). These tests have a high degree of sensitivity and specificity, but require a confirmatory test. Confirmation tests include western blot (WB) or immunofluorescent antibody assay (IFA), having higher specificity than EIA with subjective interpretations. In centralized labs, combination antigen-antibody (Ag/Ab) **(Figure 2)** tests using fourth generation enzyme or chemiluminescent immunoassay for dual detection of p24 antigen and immunodominant HIV antibodies (IgG and IgM) have facilitated near-to-patient testing to enhance the universal "test-and treat" method to reduce transmission rates[19]. One example is the Abbott's ARCHITECT® HIV Ag/Ab Combo assay (Abbott Laboratories, Abbott Park, IL) [20-22]. Improvements in sensitivity have been achieved through immunocomplex disruption or incorporation of tyramide mediated amplification systems[23]. The rapid formats of fourth generation technologies were developed to capture more window phase infections in RLSs. They have been approved recently by the FDA for

use in the US (*i.e.,* Alere's Determine™ HIV-1/2 Ag/Ab Combo; Inverness Medical, Princeton, NJ in clinics and OraQuick (R) In-Home HIV Test (FDA approved in July. 2012))[20, 24]. Generally, there are three formats of HIV Rapid Tests with two of them shown in **Figure 3A-B**: immunoconcentration (flow-through devices, e.g. Multi-Spot, Genie II, Multispot HIV-1/HIV-2), immunochromatography (lateral Flow Devices, e.g. Determine, Hema-Strip, OraQuick, Unigold) and particle agglutination (Agglutination Devices, e.g. Capillus, Serodia)[25, 26]. Also, nucleic acid-based rapid test platforms for HIV-1 testing have been developed, e.g. SAMBA[27]. Many research groups are developing sensitive and affordable systems for p24 diagnostics. One of the first applications of nanotechnology-based amplifications was reported by *Tang et al*[28] using a nanoparticle-based biobarcode amplification assay (BCA) to improve HIV-1 p24 antigen detection with a sensitivity of 0.1 pg/ml. *Parpia et al*[29] reported a low-cost dipstick p24 antigen assay (analytical sensitivity of 50 pg/mL) using a heat shock methodology for disruption of immune complexes in the plasma of infected infants, and performed visual readout to diagnose HIV in infants in RLSs[29, 30] with sensitivity of ≥ 90% and ~100% specificity[31].

Figure 3A. Example of HIV Lateral flow Rapid test. OraQuick In-Home HIV Test. OraQuick is an in-vitro diagnostic for HIV (HIV-1 and HIV-2) in oral fluid and has been FDA approved for home use. This test is based on the principle of immunochromatography and is capable of detecting HIV infection 3 months after a risk event. (www.oraquick.com, OraSure Technologies Inc.)

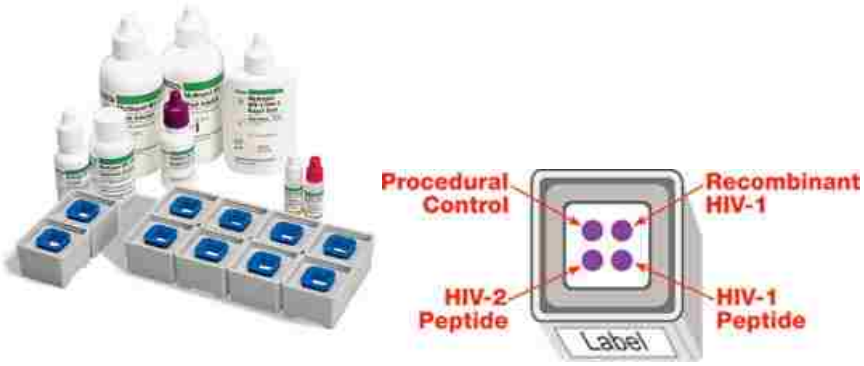

Figure 3B. Example of HIV Flow-through rapid test: Multispot HIV-1/HIV-2 Rapid Test based on the principle of ImmunoConcentration[3]. This is a rapid enzyme immunoassay to be used as a diagnostic aid for the detection and differentiation of HIV-1 and HIV-2 antibodies in human serum or plasma. (www.bio-rad.com, Bio-Rad Laboratories, Inc..)

1.3 Significance of Rapid HIV Testing

HIV screening using HIV antibody as target biomarker with "dipstick" assays represents a major improvement for POC diagnostics worldwide[32-35] [17]. However, these tests are not suitable for acute HIV infection diagnosis[32, 36, 37] given that 31% of patients who tested HIV-positive at public-sector testing sites did not return to receive their results (Centers for Disease Control and Prevention (CDC), 2000)[17]. p24 antigen is a replaceable biomarker for early HIV diagnostics because it closes the diagnostic WP. There is the possibility of saving and sustaining many lives especially in the developing countries through the development of affordable and better diagnosis devices. The World Health Organization (WHO) has outlined some characteristics (ASSURED) that must be fulfilled for devices to be considered suitable for low resources settings (Table 1).

WHO ASSURED criteria	
A	Affordable
S	Sensitive
S	Specific
U	User-friendly (simple to perform in a few steps with minimal training)
R	Robust and rapid (results available in less than 30 min)
E	Equipment-free
D	Deliverable to those who need them

Table 1. World Health Organization major desirable parameters for sexually transmitted diseases diagnostics[4].

In order to address these challenges and adapt these criteria, we have developed a low cost immunoconcentration device for sensitive detection of HIV p24 antigen using our stimuli-responsive nanomaterial-based reagent technology and non-instrumented self-powered lab card devices from PATH[38]. For the first time, **phase separation immunoassay** and **phase-change materials** have been used to develop a disposable device employing limited instrumentation making assays convenient for LRSs. Our assay is capable of accommodating a larger volume specimen (1ml), thereby improving assay sensitivity by plasma p24 antigen (found in low concentrations) enrichment. The main goal of this research was to develop a flow-through rapid testing device for HIV-1 that diagnoses p24 antigen with clinical range sensitivity (LOD ~10pg/ml))[28] similar to centralized labs tests.

The developed self-powered device can detect HIV-1 p24 antigen, helping clinicians break the infection cycle by screening for acute HIV infection earlier than conventional third generation HIV antibody tests or other current rapid tests[11]. Self-powered assays will be affordable, dependable and efficient for RLS with minimal usage training. The clinical impact of HIV rapid testing technologies in patient care will be to achieve earlier, faster infection identification, allowing immediate counseling and treatment using ARVs.

1.4 Stimuli-Responsive Reagents for Biomarker Purification and Immunoassays

Stimulus-responsive polymers respond sharply and reversibly to physical or chemical stimuli by changing their conformation and physicochemical properties, e.g., from a hydrophilic state to a more hydrophobic state[39]. The Stayton Lab at the University of Washington has pioneered new stimuli-responsive reagent systems and demonstrated important new methods for using these systems in biomolecular separation[40-54]. The reagent systems are innovative in being able to concentrate target analytes/pathogens or remove interfering molecules in simple and minimal steps that bypass the need for traditional chromatographic approaches. The reagent systems are also innovative in their controlled bioconjugation geometries, in their low molecular weight polydispersity, and in their control of compositional fidelity where copolymers are utilized. These properties facilitate effective separation and preserve the target analyte binding capability. These properties are enabled by the use of the reversible addition-fragmentation chain-transfer (RAFT) polymerization, and our group has been amongst the first to develop and use these types of controlled conjugates[46, 48-52].

Figure 4 shows an example of stimuli-responsive polymer (Poly-N-isopropylacrylamide (pNIPAAm)) solution, which exhibits a LCST at 32 ºC in water switching from a hydrophilic phase to a hydrophobic state with application of a stimulus (temperature). pNIPAAm can be conjugated to bio- and nanomaterials to perform clinically relevant diagnostic measurements[55-58]. Stimuli-responsive bioconjugates use homogeneous separation and enrichment properties to overcome the mass transport limitations associated with heterogeneous solid phase ELISA. This is because the binding of target molecules to capture ligands occurs in solution where molecular diffusion of the reagents facilitates

rapid mass transport equilibration. pNIPAAm conjugates retain the phase transition properties of the polymer to the protein and the LCST is not significantly affected after the conjugation process. The phase transition can then be exploited to separate the conjugate-analyte complex from solution enabling enrichment. This has been demonstrated with several protein-PNIPAAm systems [55, 59].

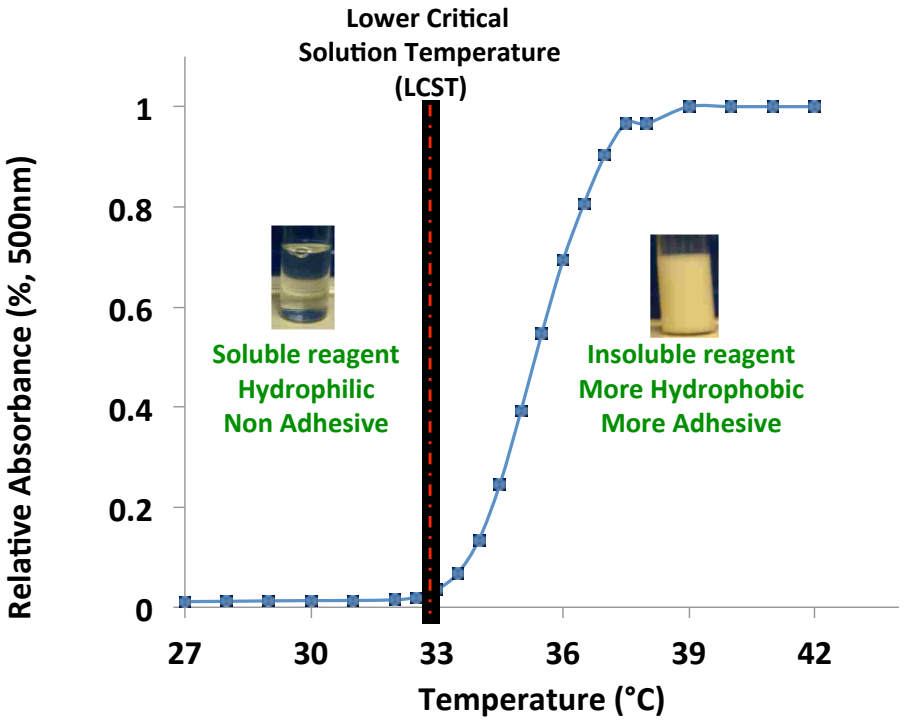

Figure 4. Scheme of stimuli-responsive polymer technology. A stimuli-response polymer exhibits a *sharp* and large response to a small stimulus (i.e. temperature). This property is readily transferred to polymer antibody conjugates.

1.5 Nanotechnology Reagents for Point-of-Care Immunoassays and Devices

Nanomaterials with desirable superior properties have been designed, synthesized, and tailored to facilitate high-performance detections for advanced immunoassays. Nanoparticles such as gold colloids, quantum dots (QDs) and carbon black are widely used for immunosensor fabrication, because of their advantages such as more freedom in orientation for protein immobilization, high surface–to-volume ratio, size tunibility, facility in electron transfer and high quantum yields. Many immunoassay methods and immunosensors are being developed for detection of tumor-related biomarkers using nanoparticles [60]. Nanoparticles can be used for sensing biomarkers and in point-of-care diagnostics and other user-friendly sensing platforms[61]. This thesis used stimuli-responsive conjugates together with gold nanoparticles (40nm) for efficient detection of p24 antigen for POC HIV diagnostics flow-through immunoassay.

We used gold colloids nanoparticles in our application because of its high molecular detection capability such as the physics governing its interaction with light on visible wavelength scale when compared to bulk-materials[62]. Some of these unique properties are: **1.** chemical functionality, **2.** surface area: volume ratio, and **3.** optical properties. Gold nanoparticles are easily functionalized and stabilized with surfactants, polymers or proteins, which give them great stability for immunoassay applications. Because assay-binding events occur at the particle surfaces, the high surface area: volume ratios give them an advantage for efficient analyte capture in bead-based diagnostics immunoassays. The optical properties of gold colloid nanoparticles that make them appropriate for optical detection applications is their large scattering cross-sections in the visible wavelengths and their tunible localized surface Plasmon resonance (LSPR)[63].

The majority of immunochromatographic ("dip-stick") assays use gold nanoparticles as the dominant detection system making them a global detection system for rapid diagnostic tests. However, the sensitivity of lateral flow tests are low because of small sample volume (Table 3), which in turn leads to overall limited absolute available biomarkers. In this thesis, we demonstrated the use of pNIPAAm-antibody conjugates to process large volumes (1ml) of HIV-1 specimen and enrich them to concentration ranges that can be detected using flow-through visual detection technologies in the presence of stimuli (**Figure 6)** without instrumentation.

1.6 Current limitations of Immunoassay Methods and POC Diagnostic Devices

The current diagnostics assay options that exhibit some of the characteristics outlined by the WHO are the Lateral Flow (Immunochromatographic) assay (LFIA) and Flow-Through (Immunoconcentration) membrane assay (FMIA) **(Table 2-3).**

Assay specifications	
Sandwich immunoassay[1]	***Lateral Flow Immunoassay[6]***
Sensitivity (LOD) (10-20pg/ml)	Sensitivity (LOD) At least 1 log worse than a similar ELISA[7]
Linear Dynamic Range ≥ 3 logs	N/A
Assay CV ≤ 15% intra-assay; ≤ 20% inter-assay	N/A
Sample: 25-200 µL of serum, plasma etc.	Sample: 5-50µL of serum, plasma etc.
Assay Format: 96-well plate/beads	Assay Format: strip
Time: 3-4 hours	Time: 5-20mins

Table 2. Comparing some assay specification of sandwich immunoassays and lateral flow immunoassays.

Table 2 compares Solid Phase Immunoassay (SPI) or sandwich ELISA to the LFIA in terms of assay specifications. The key differences that have improved with the use of LFIA are instrumentation and the reduction of long incubation times as well as the need for trained personnel. However, the limitation of small sample volume makes LFIA less sensitive than SPI.

Table 3 compares the characteristics of all 3 immunoassay formats.

Characteristics	ELISA (SPI)	Lateral Flow (LFIA)	Flow-Through (FMIA)
Assay Time	*2-4 hours*	10-20 minutes	10-20 minutes
Cost	Moderately expensive	Inexpensive Possibility of mass production	Inexpensive Possibility of mass production
Assay site Location	*Centralized laboratory*	Field Doctors offices	Field Doctors offices
Size	*Equipment dependent*	Portable device	Portable device
Storage	4C	Room temperature	Room temperature
Training and user	Trained personnel required	Little or no training User friendly	Little or no training User friendly
Specificity/sensitivity	High Specificity High Sensitive	*Low Specificity* *Low Sensitive*	*Low Specificity* *Low Sensitive*
Quantitative	High	Low Semi-quantitative	Low Semi-quantitative
Sample size (volume (µl))	*25-200*	*5-80*	>1000

Table 3. Characterization of ELISA, Lateral Flow assay and Flow-Through assays. This table summarizes some of the advantages and disadvantages of the 3 different assay principles shown in **Figure 5**.

The limitations of the systems have been outlined in **Table 2 and 3**. To address some of these limitations we have developed a flow-through membrane-based immunoassay system that combines covalently conjugated pNIPAAm-antibodies and detection conjugates in a simultaneous binding and rapid immunocomplex capture on heated porous membranes. Our approach reduces non-specific loss of protein analytes due to adsorption during long incubation periods of enzyme immunoassays (**Table 2**), which can have a major effect on assay sensitivities especially at low analyte concentrations and complex matrix systems. Secondly, in the final prototype device, we employed one step of incubation with no signal amplification compared to steps 4-6 in conventional ELISAs before signal amplification. We validated the clinically relevant sensitivity of our device in comparison with FDA approved p24 antigen ELISA (LOD=10-20pg/ml)[28].

The principles of these assay systems are shown in **Figure 5.**

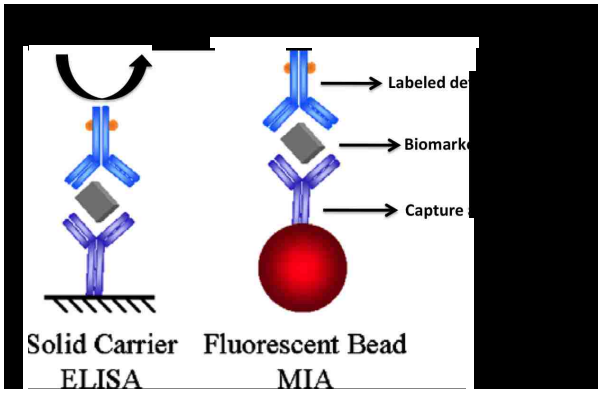

Figure 5A. Principle of solid-phase Enzyme-Linked Immunosorbent Assay (ELISA)(Adapted and modified from de Jager et al, 2006,)

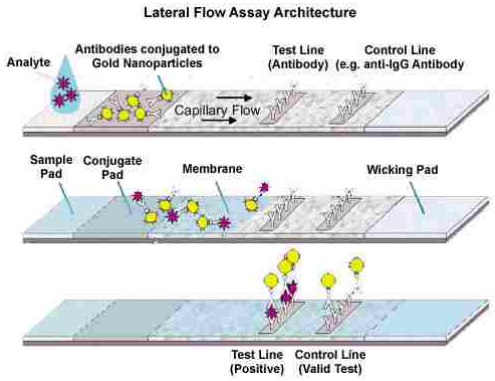

Figure 5B. Principle Lateral Flow (Immunochromatographic) assay (Adapted and modified from cytodiagnostics.com)

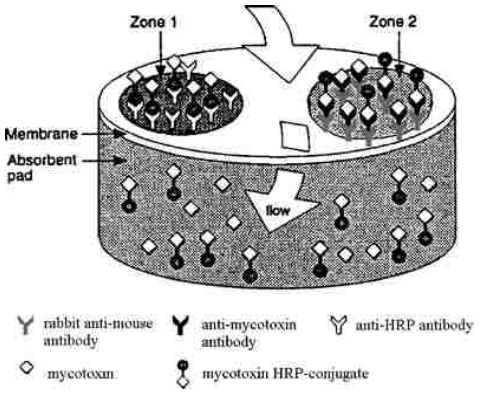

Figure 5C. Principle of Flow-Through (Immunoconcentration) assay using enzyme[5]**.** This membrane-based immunoassay technique is based on a competitive immunoassay principle and color developed is inversely proportional to the analyte concentration for the detection of ochratoxin A (OTA) in cereals and coffee.

1.6 Basic principles guiding the Development of Non-Instrumented Immunoassay Diagnostic Devices

Non-instrumented devices function through faster binding events, bio-separation, and porous diffusion and in some cases the ability for them to be self-powered when compared to some instrumented devices used for immunoassays applications in centralized laboratories.

Generally, receptor–ligand interaction **(Appendix A),** as in the case of antibody-antigen binding for solid phase immunoassay, obeys the law of mass action although the unique characteristics are different from ligand-receptor interactions that occur in solution. These include: reaction kinetics (rates and affinity), reactant volumes, actual vs functional reactant concentrations and molecular configuration of immobilized vs. solution-phase reactants[64].

Overall, these factors (i.e. diffusion dependence) are higher with solution phase interactions when compared to solid phase interactions where the time required to reach static equilibrium of the reactants is greater in the solution phase than the solid phase[64]. The interaction of antibody, biomarkers and gold nanoparticles is governed by the principle of translational diffusion.

The translational diffusivity (D_t) of a particle (i.e. antibody, gold nanoparticle) with radius (a) and viscosity (η) is defined by Stokes-Einstein Equation:

$$D_t = \frac{K_B T}{6\pi\eta a}$$

K_B = Boltzmann constant (1.38×10^{-23} JK^{-1})

T= Temperature (kelvins (K))

In this thesis we applied the concept of diffusion in our device development by studying the movement of samples across porous membranes and tubes. In particular, the disc device described in Chapter 2 used the principle of capillary action or wicking to move liquids and reagents across the porous membrane surface while in Chapters 3 and 4, the movement of liquids and reagents across the porous membrane surface could be explained by Bernoulli's principle of streamlines fluid flow within the syringe device.

Here, capillary action is defined as the movement of liquids through a permeable substance (porous membrane) due to three forces: adhesion (inter-atomic hydrogen bonding, cohesion (intra-atomic hydrogen bonding) and surface tension (tendency of water molecules to be attracted to each other caused by hydrogen bonding). Capillarity occurred when the intermolecular bonding of the liquid was significantly lower to that of the permeable substance. The equation for capillary action could be defined by:

$V = AS\sqrt{t}$

Where V = cumulative volume of absorbed liquid (ml)

A = cross-sectional area that is wetted (m^2)

S = Sorptivity of medium ($m/s^{1/2}$)

T = time (seconds)

The movement of fluids and reagent within the syringe device was guided by the Bernoulli principle or the incompressible flow equation, which describes the steady, frictionless and incompressible flows of liquids along a streamline. For a fluid with constant density, the equation is given by:

$$\frac{V^2}{2} + gZ + \frac{P}{\rho} = \text{Constant}$$

Where ρ = density of fluid at all points

P = pressure at a particular point

Z = height above a reference point opposite gravitational acceleration

g = acceleration due to gravity

V = speed of fluid flow at a particular point

This thesis focuses on the development of a non-instrumented immunoassay device for HIV-1 point-of-care diagnostic applications. Our envisioned device is shown in **Figure 6** below.

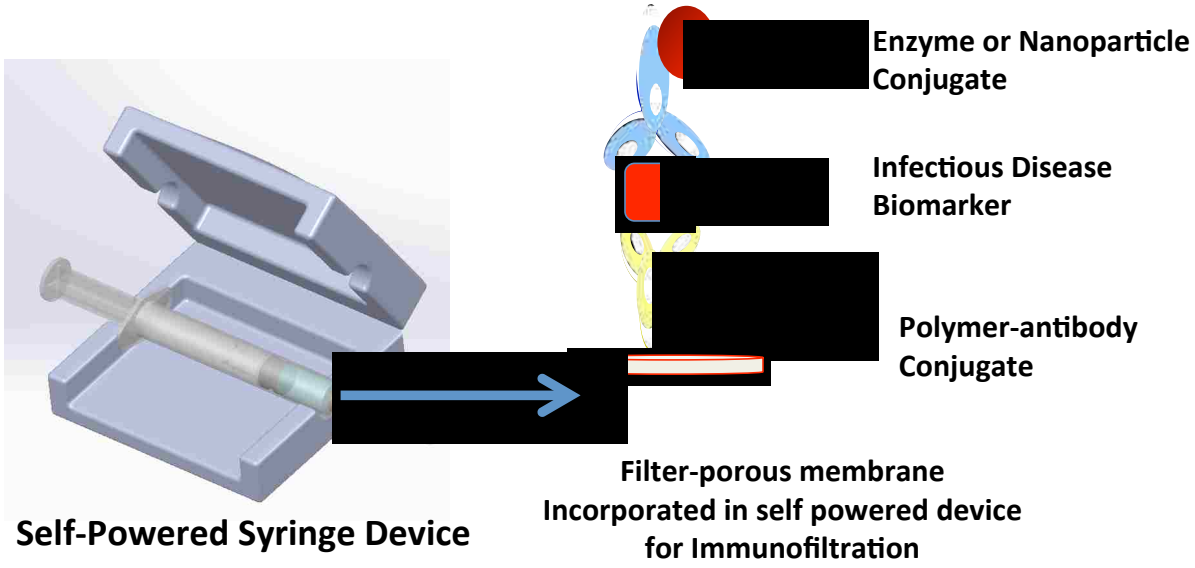

Prototype device design courtesy of LSDF Smart Card Project

Figure 6. Prototype Flow-through Device (Left) and immunoassay principle (Right). The self-powered device for rapid HIV (p24 Antigen) flow-through assay was designed using Solidworks software.

The left image in **Figure 6** is an illustration of the envisioned Self-Powered Device for Rapid HIV (p24 Antigen). The device consists of a modified Luer-lock with membrane filter (LoProdyne) attached to a 3ml syringe from BD using the Luer-lock mechanism. The syringe is wrapped around a heating pack, containing sodium acetate trihydrate in di-water (25% w/w) with a concave stainless steel chip at one end to trigger aggregation process and to generate heat. This assembly is placed in a Clamshell plastic holder, which provides pressure on the sodium acetate pouch and ensures consistency regarding the location of the syringe. The entire assembly is held tightly in position using a Velcro strip. The plunger is used to move sample in and out of syringe with device.

The right image in **Figure 6** is an illustration of the flow-through assay module and immunoassay principle. It is a rapid and simple technique for quantitative measurement of HIV p24 antigen using different detection chemistries: enzymatic reactions or nanoparticle aggregation through the formation and capture of thermally responsive immunocomplexes on the surface of a membrane using flow-through process.

For the first time, we use pNIPAAm conjugate to facilitate the development of a prototype HIV 1 diagnostic system that requires limited instrumentation, a large amount of sample, and disposable device making the assay convenient for low resource settings. We present results showing the capture and detection of biomarker immunocomplexes enhanced by covalently modified IgG antibody-pNIPAAm conjugates and unmodified nylon-6, 6 membranes inserted within a flow-through device. The formation of a dual-labeled immunocomplex sandwich in solution is specific and rapid at room temperature. The capture of immunocomplex aggregates is mediated by pNIPAAm above the LCST.

Chapter 2

Immunoassay Reagents and Flow-Through Assay Module Development

2.1 Introductions and Overview

In this chapter, we describe the development of immunoassay reagents and their detailed characterization. We focus on the robust validation of the temperature-responsive antibody conjugate ability to capture and enrich HIV-1 p24 antibody from human plasma samples specifically and selectively. We later describe the development of the flow-through membrane assay module using a controlled antibody HRP bioconjugate using a disposable flow-through disc device.

2.2 Experimental Design

We used reversible addition-fragmentation chain transfer (RAFT) polymerization to synthesize telechelic pNIPAAm followed by carbodiimide chemistry to convert its end carboxyl groups to produce highly reactive esters by reacting them with N-hydroxysuccinimide (NHS). Covalent conjugation was achieved by reacting active pNIPAAm-NHS esters with the amine groups of anti-p24 monoclonal antibody (mAb). The developed pNIPAAm conjugated anti-p24 mAb was then tested for functionality: capture efficiency, binding and specificity in solution. pNIPPAAm mediated capture of partial and full stack immunocomplexes was then performed using a vacuum manifold ELISA system and enzyme flow-through membrane immunoassay (immunoconcentration) respectively.

2.3 Materials and Methods

2.3.1 Stimuli-Responsive Capture Reagents Synthesis and Characterization

2.3.1.1 Synthesis and Characterization of pNIPAAm and pNIPAAm-NHS Ester

We synthesized telechelic pNIPAAm using reversible addition-fragmentation chain transfer (RAFT) polymerization of pNIPAAm using previously published methods **(Figure 7).** We employed AIBN as primary source of free radicals and a trithiocarbonate based ECT as chain transfer agent in 10ml of 1,4-dioxane. The polymerization was conducted at 60°C with CTA: I ratio of 10/1 under nitrogen. The CTA: Monomer ratio was 1/265 such that the theoretical Mn at 100% conversion was 30000g/mol. The purified polymer was then isolated by precipitation in pentane and characterized by Gel Permeation Chromatography (GPC) to determine their average molecular weight (Mn) and polydispersity index (PDI) against poly (methylmethacrylate) standards. Size Exclusion Chromatography (SEC) Tosoh TSK-GEL R-3000 and R-4000 columns (Tosoh Bioscience, Montgomeryville, PA) were connected in series to an Agilent 1200 series (Agilent Technologies, Santa Clara, CA) refractometer Optilab-rEX and triple-angle static light scattering detector miniDAWN TREOS (Wyatt Technology, Santa Barbara, CA). Samples were analyzed in HPLC-grade DMF containing 0.1 wt% LiBr and a mobile phase at a flow rate of 1 mL/min. The dn/dc value of the homo-pNIPAAm was determined by assuming 100% mass recovery of NIPAAm monomer.

To activate synthesized telechelic pNIPAAm to produce highly reactive esters the end carboxyl groups were reacted with N-hydroxysuccinimide (NHS) with the facilitation of 3-10% dimethylaminopyridine (DMAP) as previously reported by Neises et. al. [65] **(Figure 7).** Briefly, the reagents pNIPAAm (1 g), NHS (4.14mg) and DCC (7.42mg) in molar ratios

1:1.1:1.1 respectively were combined in 5 ml anhydrous dichloromethane at room temperature for 24 hours. After filtration of reaction byproduct N, N'-dicyclohexylurea using 0.2µm filter (Millipore), the activated polymers were then precipitated with cold anhydrous ethyl ether immediately dried by vacuum overnight before storage in desiccators at -20°C. We used spectrophotometric (λmax = 260 nm ε = 9700 $M^{-1}cm^{-1}$) analysis to confirm the presence of NHS group on polymer chains according to TECH TIP #3 protocol from Pierce (Thermo Scientific, Rockford, Il U.S.A.).

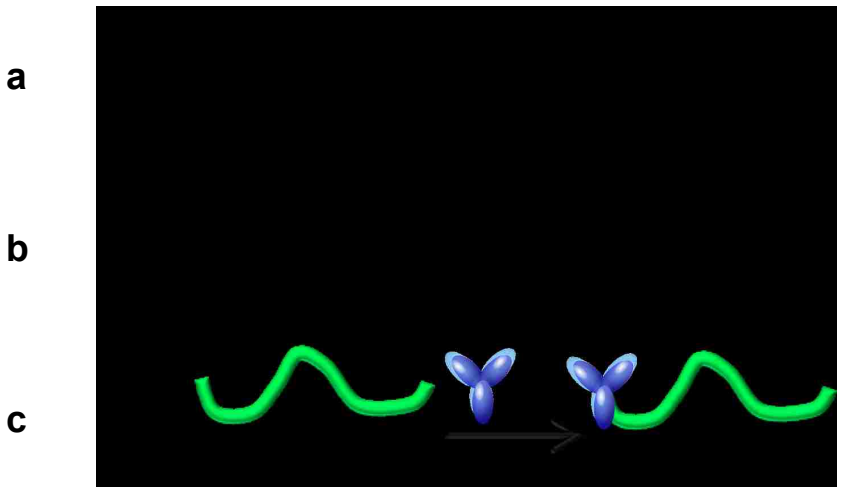

Figure 7. Scheme of pNIPAAm conjugate synthesis steps: **(a)** Synthesis of NIPAAm yielded a carboxyl terminated pNIPAAm using Reversible Addition Fragmentation Chain Transfer (RAFT) polymerization technique; **(b)** Conversion of the carboxylic end group of the pNIPAAm into N-hydroxysuccinimide (NHS) esters using carbodiimide chemistry; **(c)** Covalent conjugation of antibody to carboxylic group of activated polymers was achieved by N-hydroxysuccinimide (NHS) chemistry at pH 8.5;

2.3.1.2 Preparation, Purification and Characterization of pNIPAAm-antibody Conjugates

Covalent conjugation of antibody polymers was achieved by reacting active pNIPAAm-NHS esters with the amine groups of anti-p24 antibody (Cat # MAB739P, mAb purchased from Maine Biotechnology Inc.) at pH 8.5. NHS-activated polymers were dissolved in anhydrous DMSO and conjugation was conducted with less than 10% DMSO in the reaction medium. The molar ratio of NHS activated pNIPAAm and anti-P24 antibody was 50:1 in carbonate buffer (pH=8.5) and conjugation was performed overnight at 4°C. Unconjugated antibodies were separated from free antibodies by heating the reaction mixture to 38°C to induce pNIPAAm aggregation. Solution was gently mixed and resulting precipitate was centrifuged for five minutes at 10,000 rpm in a microcentrifuge. Supernatant was removed and the polymer pellet was re-solubilized in cold phosphate buffered saline. In order to remove free pNIPAAm from conjugated mixture, we performed ultra filtration using Amicon® Ultra-15 centrifugal filter device with 100,000Da MWCO purchased from EMD Millipore Corporation. To confirm bioconjugation, Sodium Dodecyl Sulfate PolyAcrylamide Gel Electrophoresis (SDS-PAGE) was used to separate anti-P24 antibody and its conjugates according to their electrophoretic mobility or molecular weight. Readymade gels and molecular weight markers were purchased from Bio-Rad. 5µg total protein was loaded per mini-gel well and submerged in running buffer which normally contains SDS and 1X Tris-glycine. Gels were run at 125 Volts for 1.5 hours and visualized using Gel code Blue, scanned at 1200 dpi with a Microtek Scanmaker i800 after de-staining in distilled water overnight. Final conjugate concentration was determined using a derived correction factor

for contribution of absorbance at 280nm by trithiocarbonate moiety (310nm) of pNIPAAm (**Figure 13).**

Additionally, we characterize the size and purity of bioconjugates using Size Exclusion Chromatography (SEC). Briefly, three samples (un-conjugated anti-p24 antibody, pNIPAAm-anti-p24 antibody conjugates and free pNIPAAm) were prepared in PBS pH 7.4 at concentrations >1g/l and filtered using 0.2 U filter (Fisher brand, # 09-720-3). Sample volume injected was 100ul and the running buffer used was di-water containing 0.05% NaN_3. Samples were run at a flow-rate of 1ml/min for a total of 20 minutes. The SEC system used was Viscotek (VE 3580 Ri detector, VE 3210 UV/Vis detector) and data was collected using OmniSEC 4.6.0 software.

2.3.1.3 Functionality of Bioconjugates: Capture Efficiency, Binding and Specificity pNIPAAm Conjugated Anti-p24 mAb in Solution. We evaluated the binding of p24 antigen to our conjugates by testing for free/unbound p24 antigen in a series of pretreated samples in comparison with a series of untreated samples as standards. HIV-1 p24 antigen was measured using the HIV-1 p24 ELISA kit (from PerkinElmer Life Sciences, Boston, MA). pNIPAAm-antibody conjugate binding efficiency was achieved by p24 depletion in 50% human plasma. p24 positive samples from PerkinElmer at a fixed concentration (100 pg/ml) and clinical range (10-100pg/ml) were tested. To facilitate aggregation and separation, free pNIPAAm (0.5mg/ml) was used as control and equimolar amount was added to all vials to enhance aggregation after the binding process. Sample volumes were 200µl and were tested in triplicate.

Briefly, p24 antigen was spiked in 50% human plasma provided by Valley Biomedical Inc. Conjugates were added to reaction mixture and samples incubated for 10 minutes at room temperature. After addition of free polymers, sample was then transferred into incubator (T=38-40°C) and allowed to incubate for 5 minutes until solution becomes cloudy as pNIPAAm aggregates to form white precipitate. Afterwards, the conjugates with captured p24 were spun-down using centrifuge (10k rpm for 5 minutes) under heated condition (T=38-40°C). White aggregates of conjugate with captured p24 were observed at the bottom of tube. The supernatant was collected and evaluated for p24 content using PE ELISA kit.

Triplicates of 200µl aliquots of each pretreated specimen were transferred to the ELISA plate according to the manufacturer's instructions. Both the standard and treated plates were incubated at 37°C for two hours. Wells were aspirated and washed five times with Wash Buffer (0.05% PBS/Tween 20) using Bio Tek EL406 Micro plate Washer Dispenser. After washing, 100 µl of biotinylated detector antibody was incubated at 37°C for one hour. Finally, 100 µl of Streptavidin-horseradish peroxidase (HRP) diluted at a 1:100 ratio was added for 30 minutes at room temperature followed by detection of complex by incubation with ortho-phenylenediamine-HCl (OPD) for 30 minutes. The production of a yellow color indicates positive results whose intensity (determined by optical density read at 490/630nm) was directly proportional to the amount of HIV-1 p24 captured. We further evaluated the capture efficiency by quantifying the unbound p24 antigen using PerkinElmer ELISA kit.

2.3.1.4 Capture Specificity of pNIPAAm-antibody Conjugates. We evaluated the specific capture of pNIPAAm-antibody conjugates to p24 antigen in solution and on LoProdyne membrane.

To evaluate specificity and selectivity of pNIPAAm-anti-p24 mAb conjugate to bind p24 antigen, we employed PfHRP II monoclonal (IgG and IgM) generic conjugates as alternate candidates for this evaluation. All three conjugates were synthesized using covalent linkers and Sodium Dodecyl Sulfate PolyAcrylamide Gel Electrophoresis (SDS-PAGE) confirmed conjugation and UV-VIS spectroscopy as described above. We then investigated the capture efficiency of p24 antigen as described above.

To evaluate the specific capture of pNIPAAm-antibody conjugates to p24 antigen on LoProdyne membrane, we performed an alternative, filter-based platform ELISA to illustrate the capture of smart conjugate-antigen aggregate on LoProdyne membrane. We investigated the rapid isolation of p24 antigen in solution by temperature responsive capture reagents followed by specific capture on surface of un-modified commercial nylon membrane. This experiment was designed to determine the capture efficiency of the conjugates on the membranes and the selectivity of protein biomarker (p24 antigen) to the membrane surface. Experiments were carried out at room temperature (~22°C) for binding and 40°C for capturing bound complexes. p24 antigen samples without pNIPAAm-antibody conjugates and free polymers were used as controls.

Figure 8 shows how we used the ELIFA (enzyme-linked immunoflow assay) system to study the capture of pNIPAAm-antibody conjugates with captured antigen on LoProdyne membrane during flow-through process above LCST of pNIPAAm**.**

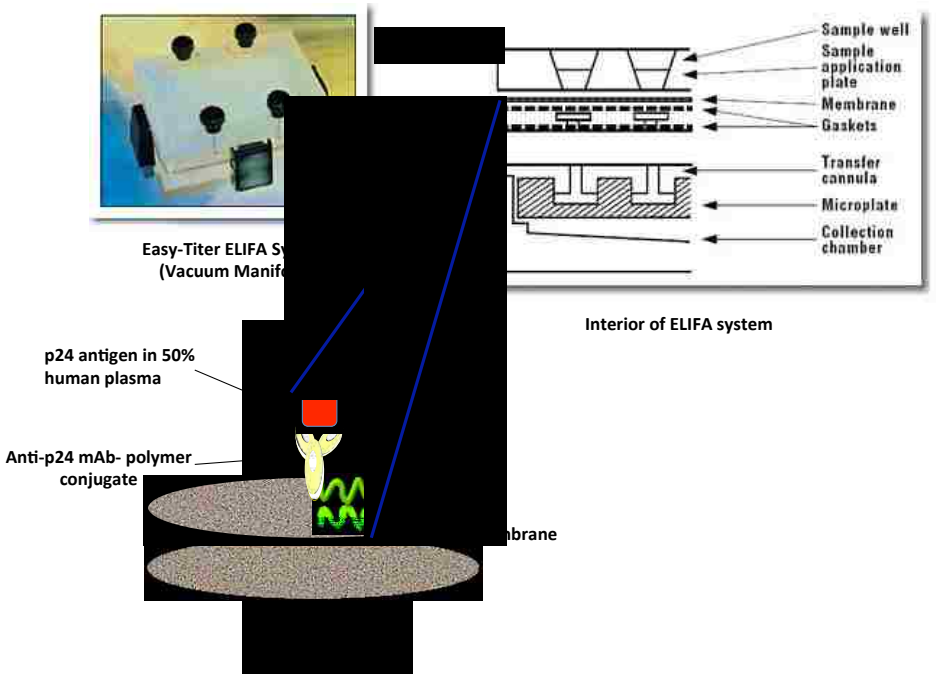

Figure 8. Scheme of Flow-through High Throughput system (ELIFA) used to characterize bioconjugates and the development of rapid enzyme immunoassay.

This system consists of a 96-well vacuum manifold for insertion of nitrocellulose or nylon membrane and can be used for dot blot immunoassays. Reactants were added to the sample application plate and a house vacuum connected to gauze was used to pull reactant through the membrane. We maintained a flow rate of 100ul/1.5minutes. The 96-well arrangement was compatible with 96-well microplates in which test samples were collected. We further evaluated the capture of partial immunocomplexes by quantifying the unbound p24 antigen using PerkinElmer ELISA kit.

2.3.2. Detection Reagent Synthesis and Characterization

2.3.2.1 Synthesis and Characterization of Anti-p24 antibody HRP Enzyme Conjugates

Anti-p24 antibody-HRP conjugates were prepared according to the protocol of EZ-Plus Activated Peroxidase kit from Pierce Biotechnology (Cat #: 31489) with major modification. We used anti-p24 antibody (NIH 3537 (Chesebro/Wehrly) from NIH. The detection antibody (Anti-p24 mAb (NIH 3537 (Chesebro/Wehrly)) was obtained as hybridoma through the AIDS Research and Reference Reagent Program, Division of AIDS, NIAID, NIH: (3537) from (Chesebro/Wehrly). Note that the hybridoma (Cat# HYB 183H125C) was used by FHCRC-BIOLOGICS for mass production of antibodies (Lot # 1116012). The amine-reactive aldehyde of HRP reacts with readily accessible primary amines of anti-p24 antibody to form covalent secondary amine bonds (imine derivatives or Schiff bases) at pH 7.2 (**Figure 9**).

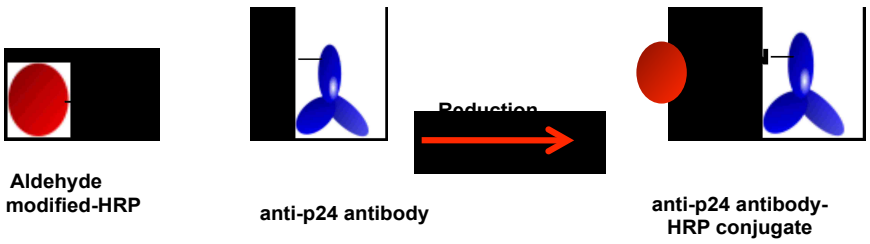

Figure 9. Reaction scheme of EZ-Plus Activated Peroxidase and anti-p24 antibody (NIH 3537). The amine-reactive aldehyde of HRP reacts with readily accessible primary amines of anti-p24 antibody to form covalent secondary amine bonds (imine derivatives or Schiff bases).

We prepared 1ml (1mg/ml) of anti-p24 antibody in PBS. In order to achieve higher conjugation efficiency, we used two vials of activated HRP per 1ml of our p24 antibody

(1mg/ml). Two lyophilized EZ-Link® Plus Activated Peroxidase (1mg per vial) was reconstituted with 100 µl of ultrapure water and immediately added to the anti-p24 antibody solution. We followed manufacturer's protocol for the remaining steps and resulting samples were purified by dialysis using a Float-A-Lyzer G2 dialysis cassette (MWCO of 100,000Da) purchased from Spectrum Laboratories, Inc., Irving TX. Samples were then stored at 4°C for characterization by BCA assay, SDS-PAGE and UV-VIS spectroscopy. Sodium Dodecyl Sulfate PolyAcrylamide Gel Electrophoresis (SDS-PAGE) was used to confirm conjugation and purification by evaluating the separation of anti-P24 mAb and its HRP conjugates according to their molecular weight as previously described. The enzyme concentration was determined spectrophotometrically, using a molar extinction coefficient of HRP at 403 nm (102000M−1 cm−1)[66, 67]. We determined p24 antibody: HRP ratio using BCA Protein assay (Product Nos. 23225) and UV-VIS Spectroscopy. For long-term storage at 20°C, we added 10mg/ml bovine serum albumin.

2.3.2.2 Binding and Specificity of HRP Conjugated Anti-p24 mAb

We evaluated the HRP conjugated antibody for binding, enzyme activity and degree of coupling (DOC). We carried out a sandwich ELISA based on commercially available anti-P24 monoclonal antibodies purchased from Maine Biotechnology Services, Portland, Maine. Here, NUNC MaxiSorp™ high protein-binding capacity polystyrene 96-well ELISA plate was coated with 1ug/ml of dilute primary anti-P24 antibody as capture antibody in coating buffer (0.1 M Sodium Carbonate, pH 9.6). Plate was sealed and incubated overnight at 4°C. Wells were aspirated and washed five times with wash buffer (PBS/0.05% Tween 20) using Bio Tek EL406 Micro Plate Washer Dispenser. Wells were blocked (3X) to prevent

non-specific binding using Superblock® Blocking Buffer purchased from Pierce Biotechnology, Rockford, lL. Washing was performed five times as outlined above and 100ul of p24 antigen (0-250pg/ml) in 50% human plasma was added to all wells. The plates were sealed and incubated at 37°C for 1.5 hour. HRP anti-p24 mAb conjugate (100 µl, 1µg/ml (NIH 3537 (Chesebro/Wehrly)) diluted in dilution buffer, pH 7.4 (PBS/2% BSA/0.05% Polysorbate 20) was added to all wells, sealed and incubated at 37°C for one hour. The plate was later washed as described above and 100 µl of soluble substrate solution 3,3', 5,5' - tetramethylbenzidine (TMB) (KPL) was added to each well and incubated at room temperature for 10 minutes in the dark. 100 µl of TMB Stop Solution was added to each well to stop the reaction and plate absorbance was read at 450nm/630nm. Curves were constructed by plotting the average absorbance value versus the p24 antigen concentration.

2.3.3 Flow-through Immunoassay Developments

2.3.3.1 Fabrication of Flow-Through Disc Devices and Immunoassay Protocols

The Disc Flow-through device was assembled using three layers of synthetic material sandwiched systematically to constitute a flow-through prototype device with diffusion capability by capillary action **(Figure 10).** A 3mm diameter hydroxyl modified LoProdyne membrane purchased from Pall Life Sciences was attached to a 1mm hole punched on a sticky plastic film. The film containing attached membrane was then placed on an absorbent pad creating a 1mm membrane surface directly on the absorbent pad for sample deposition and to enhance wicking. The immunoassay device was composed of three layers of synthetic material sandwiched systematically to constitute a flow-through prototype

device, which was placed on a heating block to provide required immunoassay temperature.

2.3.3 .2 Enzyme Flow-Through Immunoassay Protocol using Disc Device

We developed and optimized enzyme flow-through immunoassay using pNIPAAm-antibody conjugates. Details on assembly of flow-through disc device can be found in **Figure 10.** The two-step immunoassay was performed in a total reaction volume of 50ul under heated condition (T=40-42°C) in 50% spiked human plasma. For these development assays, we used a heating block (VWR Scientific, Cat # 13259-005) (in place of embedded heating pack) at constant temperature. The heating plates containing our flow-through device were heated to (T=38-40°C) for at least three minutes before the start of each experiment. Washing was performed using 2% BSA PBST at the same temperature and substrate turnover, and was terminated using di-ionized water. We evaluated non-specific signal generation for conjugates at various concentrations in 50% plasma. We evaluated the generation of background signal on membranes and the effects of washing steps in our immunoassay protocol development. Our wicking time ranged from two to four minutes. We performed the subsequent experimental step (wash step or new reagent) upon complete wicking of samples on our flow-through device. The remaining sequence of reagents was added as shown by scheme after successful wicking of the former. After developing an optimal protocol, we tested the dependence of signal on p24 antigen concentrations and constructed dose-response curves. All results were evaluated by visual inspection followed by imaging using a flatbed scanner (Micro Tek Scan Maker i800) at 2400ppi.

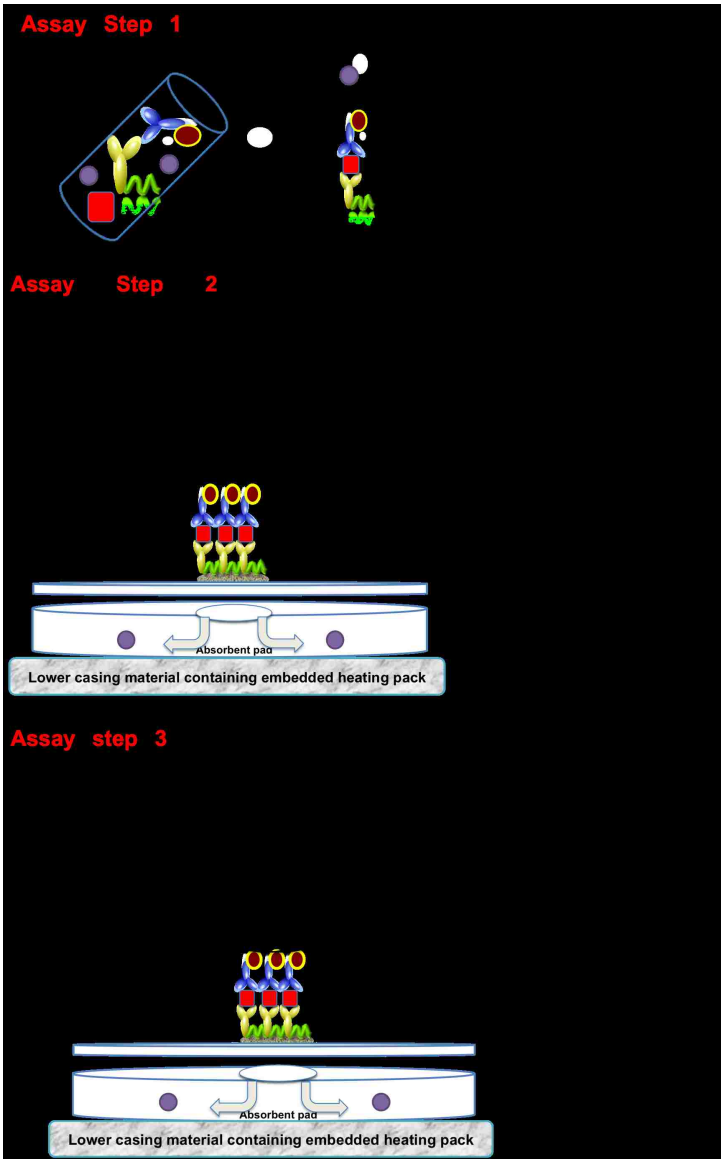

Figure 10. Scheme of enzyme flow-through immunoassay using pNIPAAm-antibody conjugates. Binding reaction was performed by incubaing samples for three minutes at room temperature to form immunocomplexes (step 1). Immunocomplex aggregation was achieved by pre-heating for three minutes at 40°C before membran capture. The washing buffer was 2% BSA in PBST (step 2). Signal was generated by adding a precipitating substrate (TMB) and the termination of enzyme-substrate reaction was achieved using deionized water (step 3).

2.4 Results and Discussion

2.4.1 Synthesis and Characterization of pNIPAAm and pNIPAAm-NHS Ester

Reversible addition-fragmentation chain transfer (RAFT) polymerization was utilized for synthesizing of the thermally responsive pNIPAAm with target Mn of 30000 Da. According to the size exclusion chromatography with multiangle light scattering detection results, the number-average molecular weight (*M*n) of the (PNIPAAm) was determined to be 23.3 kDa, polydispersity (PDI) = 1.027) and dn/dc = 0.074 **(Figure 11, Table 3).** The low PDI shows that our polymerization was well controlled. The activation of pNIPAAm into active esters via carbodiimide chemistry was confirmed by spectroscopic analysis. pNIPAAm-NHS esters reactivity was confirmed by the increase in absorbance value (λmax = 260 nm ε = 9700 $M^{-1}cm^{-1}$) of NHS-pNIPAAm solution when compared to unmodified polymer after reaction with strong base (1N NaOH) (Data not shown). This increase in absorbance was due to the intentional hydrolysis of NHS group on pNIPAAm, releasing the NHS as a leaving group that absorbs strongly at 260 nm. The active NHS-pNIPAAm esters were used for covalent conjugation to anti-p24 antibodies.

pNIPAAm	Molecular Weights (Mn) g/mol		PDIs	Conversions (%)		dn/dc
	Theoretical	Actual		Theoretical	Approx.	
P1	30000	23300	1.027	100	~78	0.074

Table 4. Molecular weights, polydispersity, and conversions of pNIPAAm synthesized by RAFT.

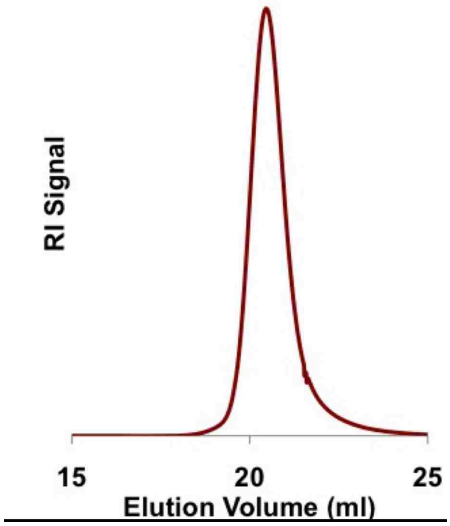

Figure 11. Refractive index GPC trace of pNIPAAm. Trace shows controlled molecular weight distribution of living radical polymerization with narrow polydispersity.

2.4.2 Preparation and purification of pNIPAAm-antibody conjugates

After successful modification of carboxylic group of temperature-responsive pNIPAAm using carbodiimide chemistry, the end group was conjugated to the primary amine group of lysine residues to anti-p24 antibodies identified by standard p24 ELISA. Successful covalent conjugation of pNIPAAm-NHS to anti-p24 antibody was verified by SDS PAGE for both crude conjugate and purified conjugate samples as shown by **Figure 12.** Because pNIPAAm is a temperature-responsive polymer that aggregates above the LCST, the resultant polymer-antibody conjugates also aggregated when the solution was heated above the LCST (**Figure 15)**. The aggregates were collected via centrifugation, which allows the removal of unconjugated antibodies. SDS PAGE showed successful conjugation

and purification thereby confirming covalent bioconjugation of NHS activated pNIPAAm to p24 antibody. Purified pNIPAAm-antibody conjugate showed a decrease in electrophoretic mobility when compared to unconjugated antibody **(Figure 12).** The smeared band (lane 4) represented the conjugated antibody. Purified conjugates were quantified using a correction factor for contribution of absorbance at 280nm by the trithiocarbonate moiety of pNIPAAm, as previously described by Golden et al [55] (Figure 13). The LCST of pNIPAAm antibody conjugate was determined to range from 34-42°C.

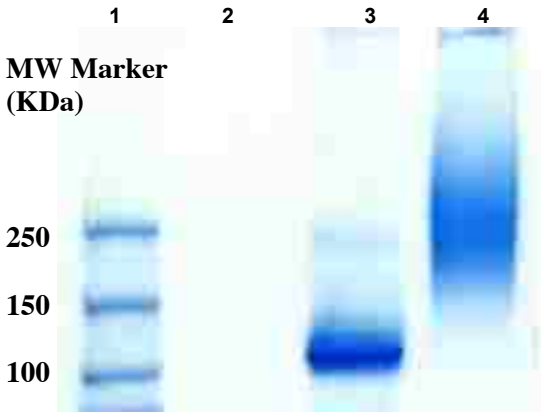

Figure 12A. SDS-PAGE gel of thermally responsive pNIPAAm antibody conjugate. Lane 1 Molecular weight marker; Lane 2 pNIPAAm; Lane 3 anti-p24 antibody; Lane 4 anti-p24 antibody conjugate. Equimolar amounts of protein were used and proteins were separated based on size by electrophoretic mobility prior to staining with gel code blue. It can be seen that conjugate moved slower across the gel due to increase in size as a result of conjugated pNIPAAm when compared to the antibody.

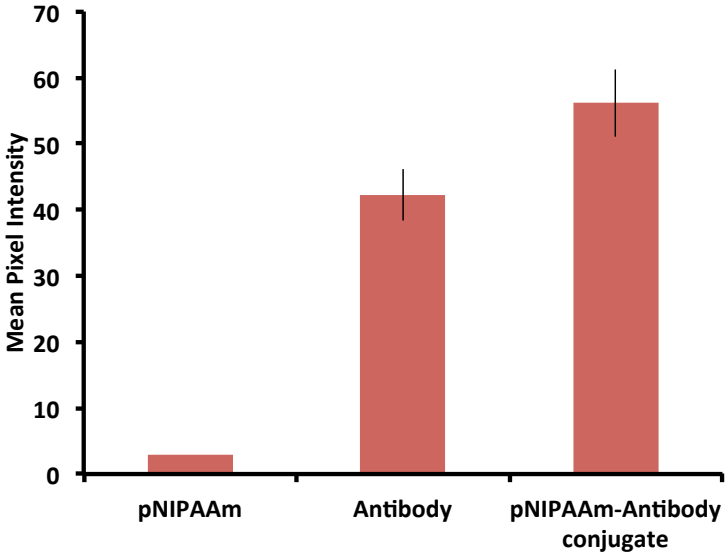

Figure 12B. Line densitometry analysis of SDS-PAGE gels (n=6). Equi-dimensional boxes were placed on lanes containing pNIPAAm, antibody and conjugate and pixel intensity of inverted images was measured using Image J. We observed increasing intensities from pNIPAAm-antibody conjugate > Antibody > pNIPAAm and results were consistent for 6 different conjugation processes.

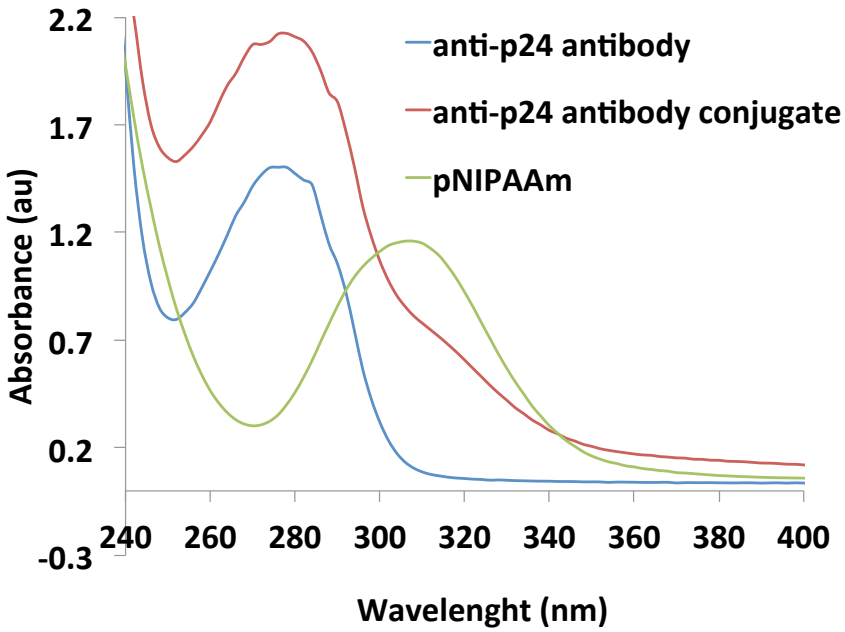

Figure 13. UV/Vis spectroscopy of pNIPAAm, antibody and pNIPAAm-antibody conjugate. Purified conjugates were quantified using a correction factor for contribution of absorbance at 280nm by the trithiocarbonate moiety of pNIPAAm at 310nm as shown by the distinct peaks.

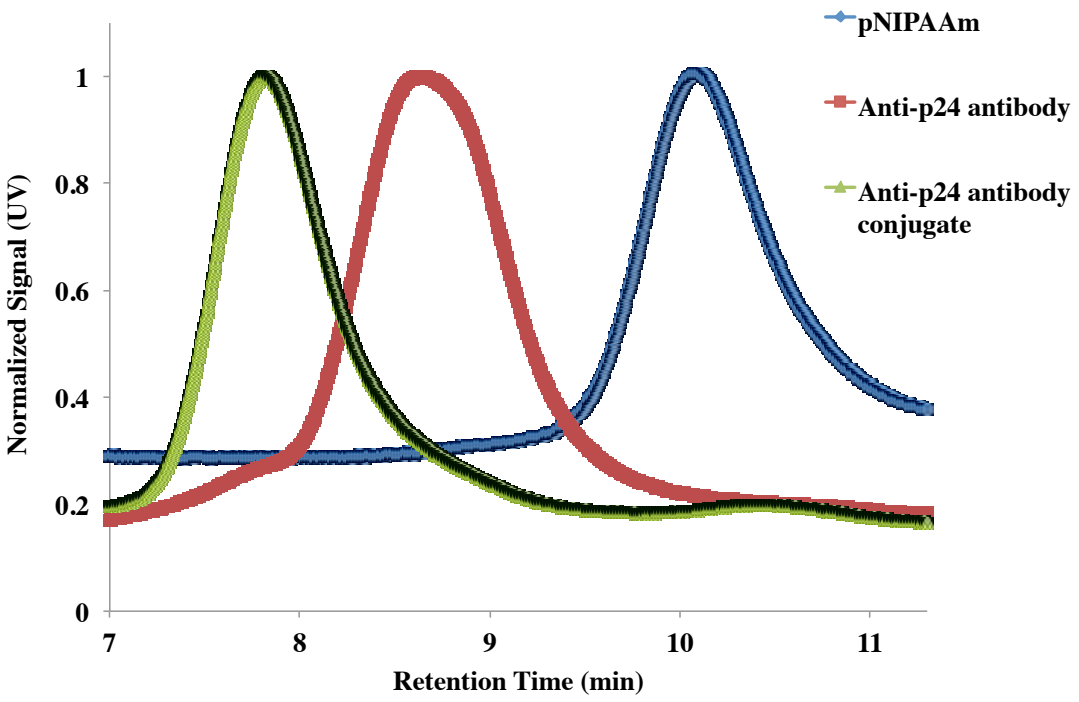

Figure 14. Size-exclusion chromatography (SEC) of anti-p24 antibody conjugate. Chromatograms show the normalized UV absorbance profile as measured at 280 nm (arbitrary units not indicated) versus the elution time of the pNIPAAm (blue), anti-p24 antibody (red) and anti-p24 antibody conjugate (green). The conjugate elutes well before the antibody and the pNIPAAm, which indicates that conjugate contains some pNIPAAm chains on its surface.

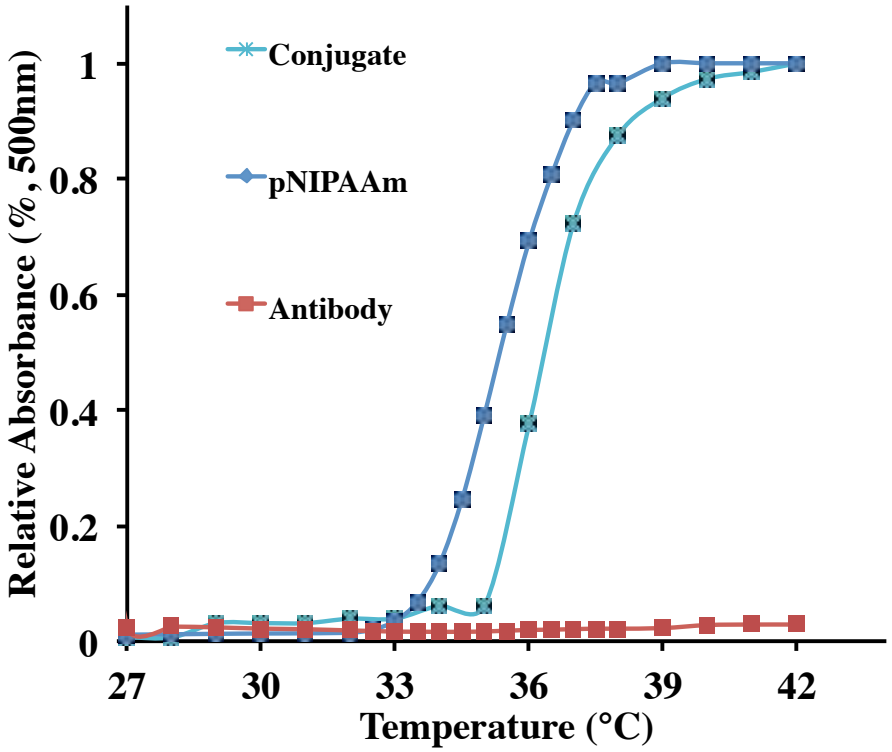

Figure 15. LCST behavior of polymer and polymer-antibody conjugate. Turbidity (cloud point) measurements at 500nm of pNIPAAm and pNIPAAm conjugates were used to monitor aggregation between temperatures 27-42°C. The gradual increase in temperature led to the increase in entropy causing the water molecules to escape into the solution and the hydrophobic pNIPAAm chains of both free pNIPAAm and pNIPAAm antibody conjugate to aggregate. The lower critical solution temperature (LCST) behavior of samples was measured by monitoring their absorbance with a HP8452 Diode Array Spectrometer containing a jacketed cuvette holder used to control the temperature. Temperatures were increased at the rate of 1.2°C /min and the solution absorbance at 500nm was recorded at 1°C interval.

2.4.3 Functionality of pNIPAAm Conjugated Anti-p24 mAb: Capture Efficiency, Binding and Specificity

The ability of the pNIPAAm-antibody conjugates to specifically capture p24 antigen with high efficiency in solution is critical for pNIPAAm mediated p24 antigen immunoassay. This experiment was designed to evaluate the retention of anti-p24 mAb functionality after bioconjugation. We also evaluated the temperature responsiveness of the attached pNIPAAm chains, and determined the minimum amount of thermally responsive p24 antibody conjugates required for binding ≥80% of p24 antigen within a clinically relevant range (10-100 pg/ml). **Figure 16** shows results from a depletion assay with p24 antibody conjugates. Quantification of unbound p24 antigen in the supernatant was done with ELISA. The fractions were calculated using mass balance. The amount of free p24 antigen was calculated using equation obtained by linear regression (R=99%) of positive samples of PE ELISA kit. The results in **Figure 16** indicate that we were able to capture ~85% of 100pg/ml p24 antigen from solution with conjugate molar excess ≥1000. In a similar approach, we used thermal precipitation and separation by centrifugation to evaluate capture efficiency across clinical range of p24 antigen (data not shown). In both cases, we were able to achieve ~90% capture efficiency of p24 antigen with (polymer conjugate molar excess ≥1000) concentrations as low as 10pg/ml and as high as 100pg/ml. This result is compatible with binding model as outlined in Appendix A ($Kd=10^{-9}M$). Conjugation of pNIPAAm to antibody does not affect binding of p24 antigen to the polymer conjugate and pNIPAAm remains temperature-responsive after bioconjugation (**Figure 15)**.

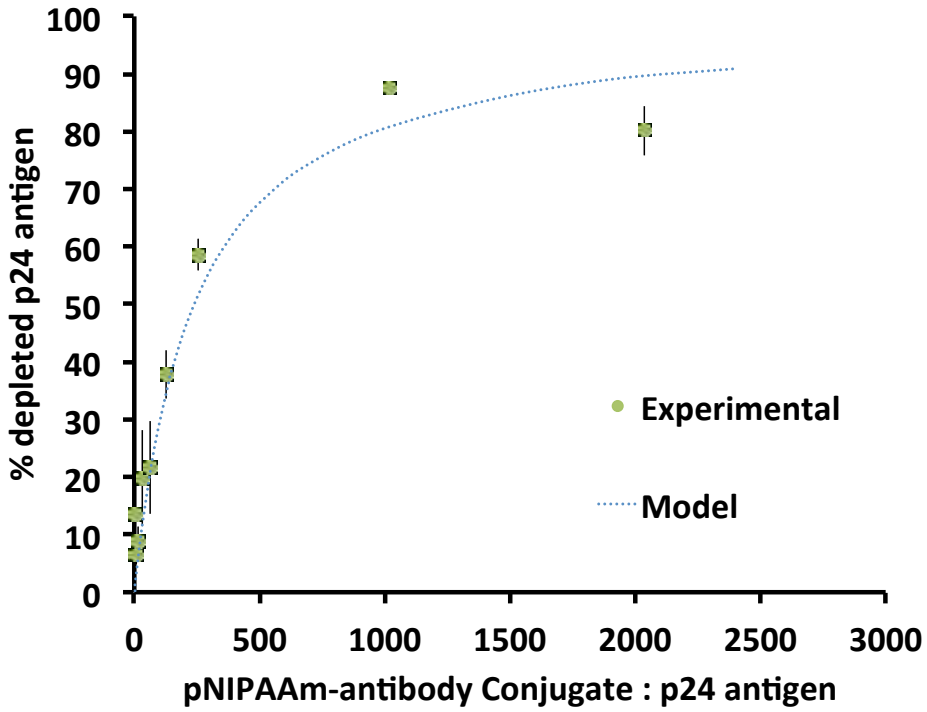

Figure 16. Binding curve of anti-p24 pNIPAAm conjugates. Model binding curve was constructed using Mathematica software at Kd=10^{-9}M, constant p24 antigen concentration and variable anti-p24 conjugate concentration. Experimental binding results show the variation in fraction of bound p24 antigen (100pg/ml = 4.18pM) at various molar ratios of Ab: p24 antigen. Samples were treated with different amounts of antibody conjugates, subjected to heat above LCST to induce pNIPAAm aggregation and separated by centrifugation. Quantification of unbound p24 antigen in the supernatant was done with ELISA. We achieved >80% capture efficiency when anti-p24 antibody conjugates are in >1000 molar excess. Data represent mean of triplicates and error bars indicate standard deviation.

2.4.4 Capture specificity of pNIPAAm-antibody Conjugates

The specificity and selectivity of immunoassay reagents is critical for prevention of low signal-to-noise ratios (S/N) and false positives. **Figure 17** shows the results obtained from the specificity studies of pNIPAAm bioconjugate. Prior to these studies, we verified the reactivity within clinical range of pf-HRP II IgG capture antibody, which we used for conjugate construction (data not shown). The ability of the IgM antibody to bind pf-HRP II was also tested. The current results (**Figure 17**) show that only anti-p24 conjugate was able to capture ~90% p24 antigen (100pg/ml) in 50% human plasma. The active pf-HRP II conjugates (IgG and IgM) did not bind p24 antigen. This shows that only NIPAAm-modified anti-p24-mAb will specifically isolate and separate p24 antigen from solution. This demonstrated the specificity of captured anti-p24 mAb conjugates and confirmed that bioconjugation does not disrupt the binding pocket of anti-p24-mAb. Also, p24 depletion was not mediated by non-specific aggregation of biomolecules and free pNIPAAm in plasma.

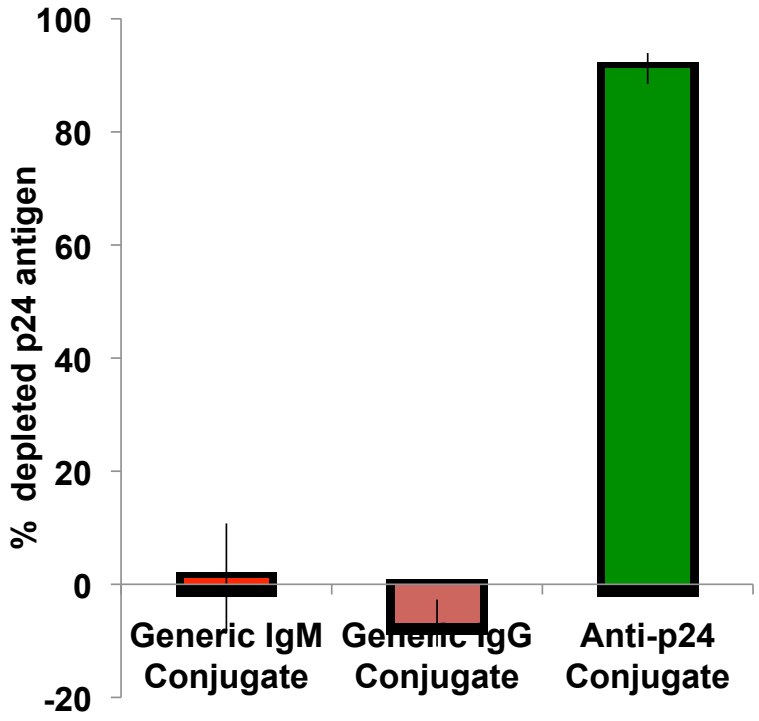

Figure 17. Specificity of pNIPAAm-anti-p24 conjugate to p24 antigen. The result shows the variation of % depletion of 100pg/ml p24 antigen with different species of temperature responsive conjugates (p24 antigen: pNIPAAm conjugate 1:2000). Samples were treated with different three polymer antibody conjugates, subjected to heat above LCST to induce pNIPAAm aggregation and separated by centrifugation. Quantification of unbound p24 antigen in the supernatant was done with PE kit p24 antigen ELISA. It can be seen that only anti-p24 conjugate could be captured ~90% p24 antigen (100pg/ml) in 50% human plasma. The pf-HRP II conjugates (IgG and IgM) did not bind p24 antigen. Data represent mean of triplicates and error bars indicate standard deviation.

2.4.5 Capture efficiency of p24 antigen on the membrane

Here, we designed experiments to demonstrate specific capture of half-sandwich immunocomplexes on nylon membranes and methods to study non-specific capture of p24 antigen on our membrane. The ability of pNIPAAm-p24 antibody conjugates with bound p24 antigen to form aggregates at temperatures above LCST would lead to their capture on LoProdyne membrane through hydrophobic interactions. During the flow-through process, hydrophobic interaction between collapsed pNIPAAm and hydrophobic unmodified nylon membrane will lead to immobilization of aggregates on membrane surface. **Figure 18** shows the results obtained from the quantification of free/unbound p24 antigen in supernatant of samples flown across LoProdyne membranes above LCST of pNIPAAm using the PE ELISA kit. The curve shows the variation of amount of p24 antigen with fraction of bound p24 antigen. All samples were run in triplicates. The fractions were calculated using mass balance. The amount of free p24 antigen was calculated using equation obtained by linear regression (R=99%) of positive samples of PE ELISA kit. The amount of conjugate used was 12nM. The results show that ~ 90% of the p24 antigen was no longer present in the collected sample tested using ELISA. The presence of our polymer conjugate (binding) and the filtration process (ELIFA) led to the reduction of our initial amount of p24 antigen. From these results, we were able to conclude that p24 antigen alone does bind to LoProdyne membrane non-specifically and partial immunocomplexes of pNIPAAm anti-p24 conjugates and p24 antigen were captured on membrane (**Figure 18)**. This bound complex can be separated by membrane-mediated capture above LCST of pNIPAAm through immunofiltration and the supernatant obtained used to calculate the fraction of bound p24 antigen. This experimental result is comparable to the previous depletion assay

method (binding followed by thermal separation through centrifugation of 100pg/ml p24 antigen) (**Figure 16**). We saw that we were able to deplete ~>80% of our p24 antigen as compared to ~95% through membrane depletion. Our result in **Figures 17 and 18** confirms that we can bind, isolate and separate p24 in solution if we spin down or use a high throughput ELIFA system to capture semi-sandwich aggregates and analyze the supernatant or flow-through solution respectively.

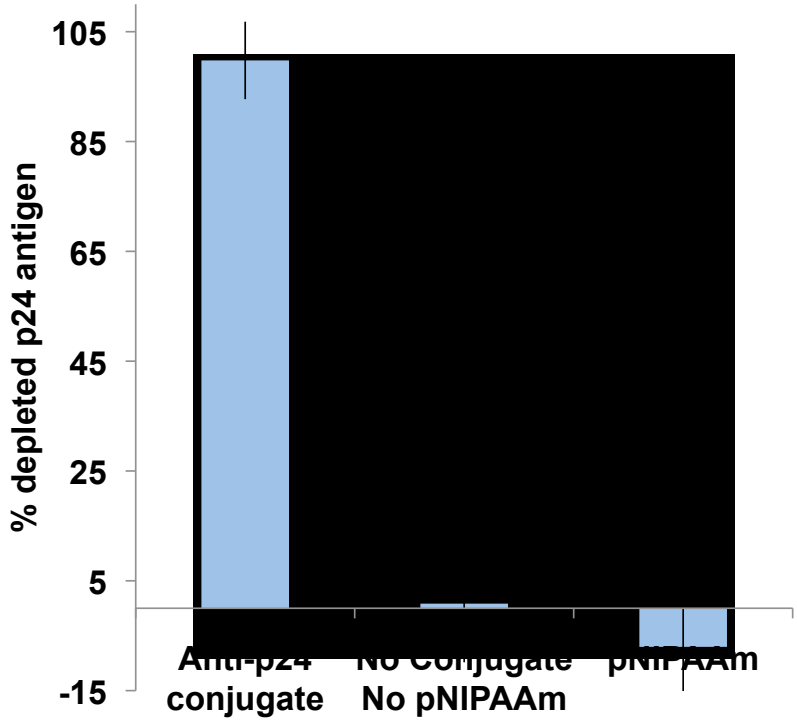

Figure 18. p24 capture efficiency on LoProdyne membrane via pNIPAAm-antibody conjugates. p24 antigen samples (10pg/ml) in 50% plasma was treated with pNIPAAm polymer/pNIPAAm conjugate (>2000 molar excess of conjugate) and flown through filter (LoProdyne membrane). Binding reaction was performed at room temperature by incubating samples for 10 minutes followed by aggregates formation by pre-heating for three minutes at 40°C. The ELIFA system used allowed us to collect flow-through samples into a 96-well microplate. The flow rate was maintained at 100ul/1.5minutes. The collected flow-through solutions were evaluated for p24 antigen content using PE kit p24 antigen ELISA. Results show that >95% p24 antigen was recovered in the supernatant of the control sample and sample treated with pNIPAAm. Data represent mean of triplicates and error bars indicate standard deviation.

2.4.6 Synthesis and Characterization of Anti-p24 antibody HRP Enzyme Conjugates

The plus activated amine-reactive horseradish peroxidase (HRP) was expected to couple with p24 antibodies to form covalent secondary amine bonds. This was confirmed by SDS-PAGE where the conjugate bands showed a complete shift in molecular weight when compared to activated HRP and anti-p24 antibody (data not shown). This conjugate, however, contained an excess of activated HRP as expected. The unconjugated activated HRP were removed by dialysis to yield a pure conjugate. The results of the gel coupled with BCA assay showed that we were able to retain the majority of our HRP conjugates during the dialysis process. Similarly, we used UV/VIS spectroscopy to monitor the removal of unreacted active HRP. The disappearance of HRP peak (~403nm) showed that the free activated HRP was removed during dialysis. The increase in the absorbance of conjugates also confirmed that we had conjugates given that both antibody and enzyme are proteins and will absorb light at 280nm.

To further characterize our conjugates, we used the total amount of protein Bicinchoninic Acid Assay (BCA assay) and the amount of HRP ($£_{403\ nm}$ = 2 for a 1-mg/ml HRP solution) to estimate the degree of coupling or number of HRP/mole IgG. Using mass balance and the known molecular weights for anti-p24 antibody (IgG, MW = 150,000Da) and HRP (MW = 40,000Da), we calculated the average number of HRP moieties per anti-p24 antibody molecules.

To evaluate enzyme conjugates ability to bind p24 antigen we studied enzyme conjugates' binding against p24 using solid phase sandwich ELISA. This is because p24 antibody conjugated to HRP can bind p24 antigen in a test solution or solid phase to form an immunocomplex. The degradation of the enzyme substrate, which is quantified

photometrically, is proportional to the concentration of the unknown "antibody" or "antigen" tested[68]. p24 ELISA with antibody conjugated with HRP showed variation of absorbance with p24 antigen concentration (red spots, **Figure 19**). Spiked p24 antigen in 50% human plasma was used to test the activity of the HRP conjugate (p24 antigen LOD=21.54 pg/ml) (**Figure 19**).

The increase in absorbance values with increasing p24 antigen was an indication that our anti-p24 antibody conjugate retained its functionality (binding) and contained HRP (enzyme activity). The antibody retained binding capability and the HRP retained activity for use in flow-through immunoassay applications.

In summary, the aldehyde groups of activated HRP were covalently conjugated to primary amines on the monoclonal antibody to form a new anti-p24 HRP conjugate. This conjugate contained 2 HRP per anti-p24 antibody and was effectively purified by dialysis. The antibody retained binding capability and the HRP retained activity for use in flow-through immunoassay applications.

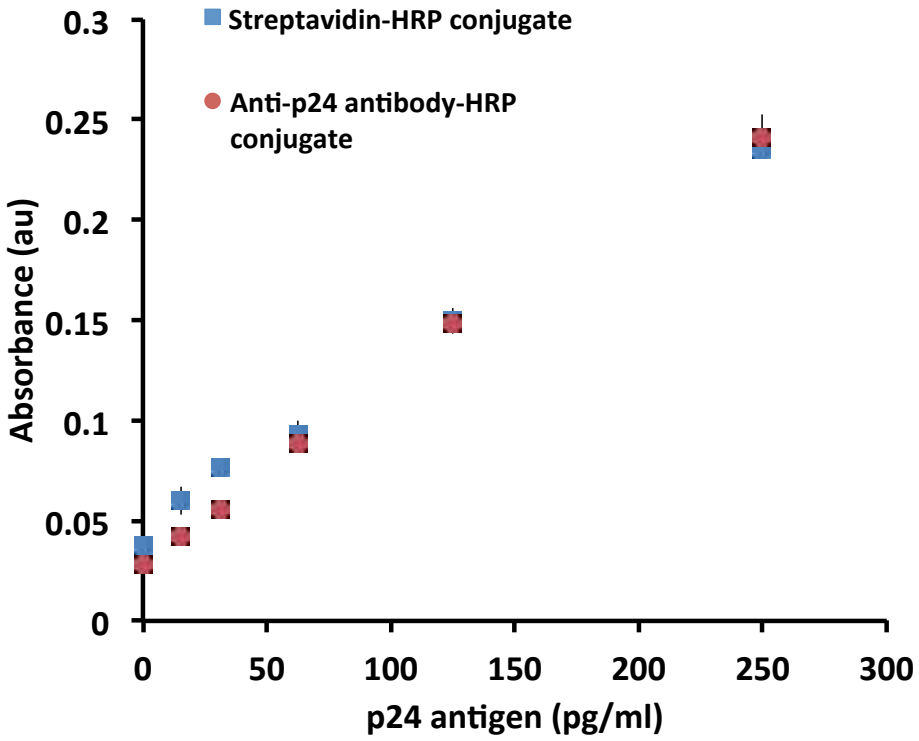

Figure 19. ELISA results showing variation of absorbance with p24 antigen concentration using developed HRP conjugate. Spiked p24 antigen in 50% human plasma was added to 1ug/ml plated anti-p24 antibody from Maine Biotechnology. 1ug/ml HRP conjugated antibodies were used to confirm the dependence in concentration of these HRP conjugates to p24 antigen concentration. As a control/reference, Streptavidin-HRP conjugate (blue dots) was used following the same protocol. The lower limits of detection (LOD) for p24 antigen were 21.54pg/ml and 24.82pg/ml for HRP conjugated antibodies and Streptavidin-HRP conjugates ELISAs respectively.

2.4.7 Development and Optimization of Enzyme Flow-Through Immunoassay using Polymer Conjugates

The flow-through membrane-based immunoassay system combines covalently conjugated pNIPAAm-conjugated antibodies and enzyme conjugates in a simultaneous binding and rapid immunocomplex capture on hydrophobic heated membranes. Thermally responsive immunocomplexes of HIV-1 p24 antigen labeled with HRP in 50% human plasma samples were captured on hydrophobic membranes and detected using TMB precipitating substrates. **Figures 20?a, b, and c** shows the dose-response curve result from the optimized titration. We observed an increase in visible signal as we increase p24 antigen concentration. We observed no background signal with our zero samples. The visible spots on all samples were imaged using a flatbed scanner and all dots were analyzed using Image J. We obtained mean pixel intensity for each p24 antigen value, which we used for semi-quantitative data analysis. This has shown positive detection of 10pg/ml of HIV-1 p24 antigen in 50% human plasma and the assay was performed in less than 20 minutes with COV <10%. This rapid test is better than the current ELISA systems, which requires several hours of incubation and amplification steps. This system provides rapid immunocomplex capture and detection for application to HIV-1 p24 antigen immunoassay without a solid support. The developed flow-through immunoassay is a promising screening system for p24 antigen and possibly for other infectious disease biomarkers for low resource settings.

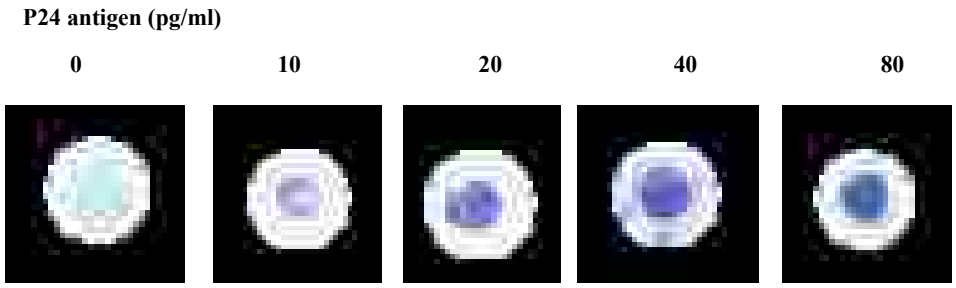

Figure 20A. Results and membrane images of rapid flow-through ELISA. (A) Flatbed scans images showing visible signals at different p24 antigen concentrations. pNIPAAm conjugates and HRP conjugates were added to 25µl sample of variable p24 antigen spiked in 50% human plasma. Samples were incubated and pre-heated for three minutes sequentially before addition to flow-through device. After washing with PBST, 0.05% Tween-20, 2% BSA, TMB membrane substrate was added to 1mm spot. Deionized water was used to stop reaction.

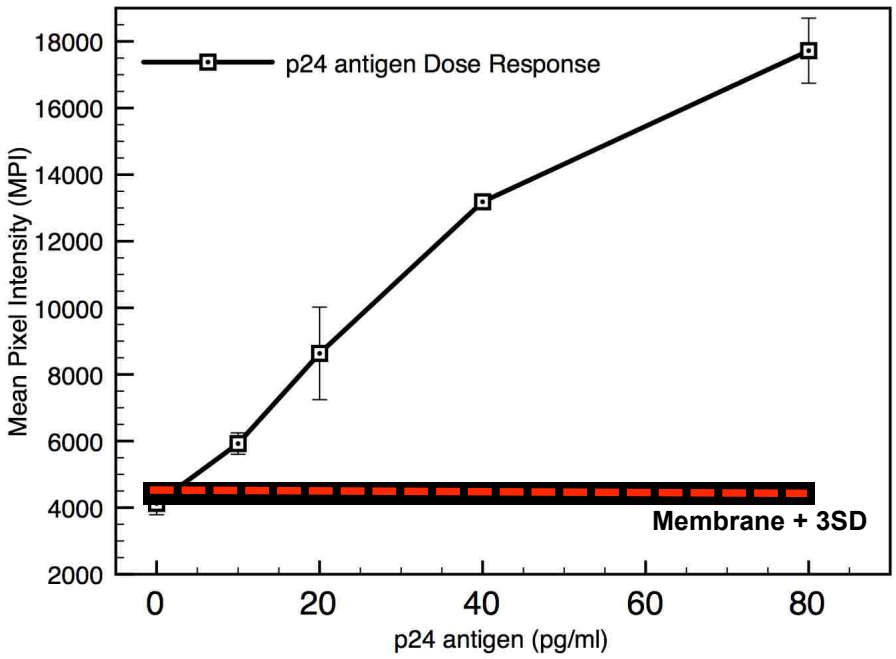

Figure 20B. Dose response curve of p24 antigen from spiked human plasma samples. The spots shown in **Figure 20A** were analyzed using image J to obtain mean pixel intensity (MPI) of the circular regions of interest. The spot area was kept constant (1mm) for all measurements and MPI measured. The averages of MPI values were plotted against p24 antigen concentrations. The error bar represents standard error for four independent samples.

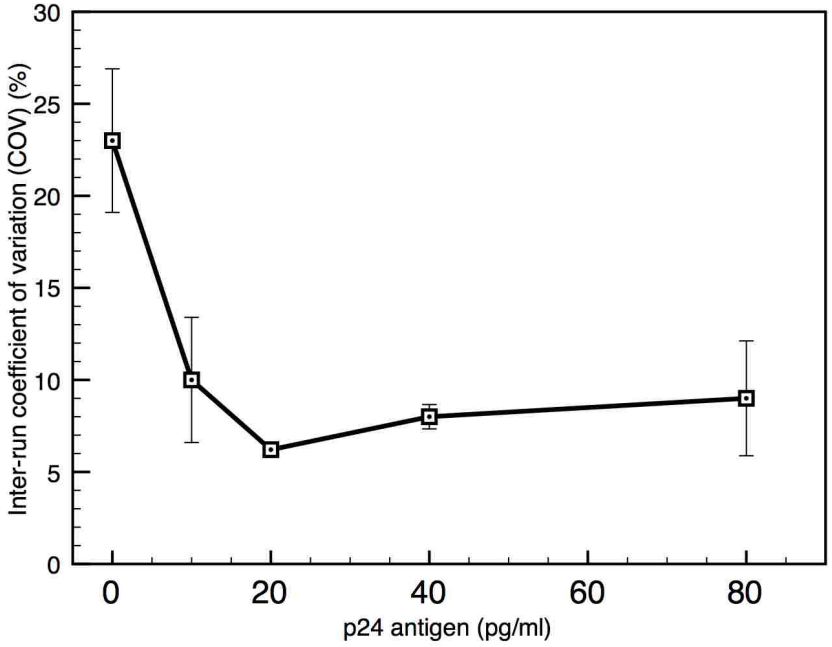

Figure 20C. Inter-run coefficient of variation (COV) of independent rapid flow-through ELISA. Flow-through immunoassay was performed as described in **Figure** 20A above. MPI of dot blots was determined at different p24 antigen concentrations as previously described. The CV at each p24 antigen concentration was calculated by dividing the standard deviations of the 8 independent samples.

2.5 Conclusion

We have developed a flow-through membrane based immunoassay system that combines covalently conjugated pNIPAAm-conjugated antibodies and enzyme conjugates in a simultaneous binding and rapid immunocomplex capture on hydrophobic heated membranes. Rapid detection of captured target was facilitated by a precipitating substrate

on membrane surface for visualization and semi-quantification. This new rapid flow-through ELISA system was facilitated by the ability of pNIPAAm antibody conjugates to bind antigen in solution.

Specifically, temperature-responsive immunocomplexes of HIV-1 p24 antigen labeled with HRP in 50% human plasma samples were captured on hydrophobic membranes and detected using TMB precipitating substrates. The LOD was 10pg/ml in 50% human plasma and the assay was performed in less than 30 minutes. This rapid test is better than the current ELISA systems, which require several hours and an amplification step.

In summary we developed a flow-through membrane module for isolating and detecting HIV-1 p24 antigen at clinically relevant concentrations using pNIPAAm-antibody conjugates. This system provides rapid immunocomplex capture and detection for application to HIV-1 p24 antigen immunoassay. The developed flow-through immunoassay is a promising screening system for p24 antigen and possibly for other infectious disease biomarkers for low resource settings. Changing detection reagent to gold nanoparticle to overcome low resources conditions such as storage and reducing overall assay steps to improve this diagnostic platform was the subsequent next step in this thesis. We then employed a non-instrumented device to supply the heat needed for temperature-responsive immunocomplexes aggregation to help overcome the technological barriers to make assay adaptable for RLSs.

ACKNOWLEDGMENTS

The next two chapters are focused on the development of the non-instrumented prototype device design courtesy of LSDF Smart Card Project team members: Dr. Patrick Stayton, Dr. James Lai, Dr. Gonzalo Domingo, Dr. Bernhard H Weigl, Paul LaBarre, Daniel Stevens, Jeremy Capalungan, Jered Singleton and Shawn McGuire. The author performed all the experiments, collected and analyzed all the data.

Also, the author will like to acknowledgement the NCI NIH T32 training grant (T32CA138312) for their support during the academic year 2012/2013 while he worked on this thesis.

Chapter 3

Non-Instrumented Syringe Device and Gold labeled Flow-Through Assay Development

3.1 Introductions and Overview

In Chapter 2 we demonstrated that polymer antibody conjugates can bind p24 antigen in solution with greater than 80% capture efficiency. We also demonstrated flow-through immunoassay in plasma-spiked samples with the capture of the p24 immunocomplex on the membranes using enzyme conjugates (LOD ~10pg/ml) with reproducibility capabilities <10%.

In this chapter we will describe the development of non-instrumented syringe device and heat generation module to replace the heating block used in Chapter 2 above. Using this broadband prototype device we will develop a flow-through immunoassay for plasma-spiked samples with capture of the p24 immunocomplex in a syringe device on the membranes using gold nanoparticle conjugates. We will evaluate the assay performance in the syringe device using individual plasma spiked samples with different anti-coagulants (e.g., sodium and potassium EDTA). The specificity of the assay will be evaluated using a panel of individualized specimens known to be HIV-negative.

3.2 Experimental Design

The main objective of this chapter was to develop a heater with plastic holder configuration using Phase Change Materials (PCMs) and assay parameters identified in **Table 5**. We designed a functional self-powered prototype device with the required immunoassay targeted temperature and demonstrated the polymer antibody conjugate aggregation and

bioseparation using the device. The performance of the device matched the parameters that were achieved using heating blocks or incubators both in terms of required reagent amount and activity as well as assay parameters.

The Non-Instrumented syringe device was fabricated using plastic materials through molding and printing. The material used to develop the prototype device was Rigid Opaque black material (VeroBlackPlus RGD875, Stratasys, Ltd). These materials were from a family of photopolymers with excellent detail visualization and capabilities for accurate 3D printing for realistic prototypes devices. A Versatile desktop 3D printer (Objet30 Pro, Stratasys, Ltd) was used for molding and printing.

Next, we developed a heating module using PCMs and reaction conditions to identify the combination of exothermic reaction temperatures capable of maintaining device temperature at 40±3°C for 30 minutes. We tested the device for temperature generation, polymer aggregation and specific capture of polymer antibody conjugate with bound p24 antigen. We then developed a gold-labeled flow-though immunoassay using this prototype device, and evaluated its specificity and selectivity to individualized plasma samples.

3.3 Materials and Methods

3.3.1 Non-Instrumented Syringe Device Design Specification

The initial prototype device was made up of five individual components (**Figure 21**). **(1.)** The membrane holder (female luer-lock fitting (P-618)) was made out of polypropylene (1/4-28) and was purchased from IDEX Health and Science. This device was modified by cutting out 1mm of polypropylene from the shoulder height to ensure accurate fitting to syringe and prevent any leakage of sample. The membrane filter (LoProdyne, 1.2 µm pore

size) was inserted into a modified luer-lock fitting as a membrane holder before device assembly. The fitting with inserted membrane is attached to **(2.)** 3ml syringe from BD by luer-lock mechanism. (**3.)** 2D bent plastic holder. **(4)** Heating Pouch. The heating source is made up of Phase Change Material (PCM) that is sodium acetate trihydrate in di-water (see Section 3.3.2 for details). This reusable heater pack was designed to fit as a syringe receptacle.

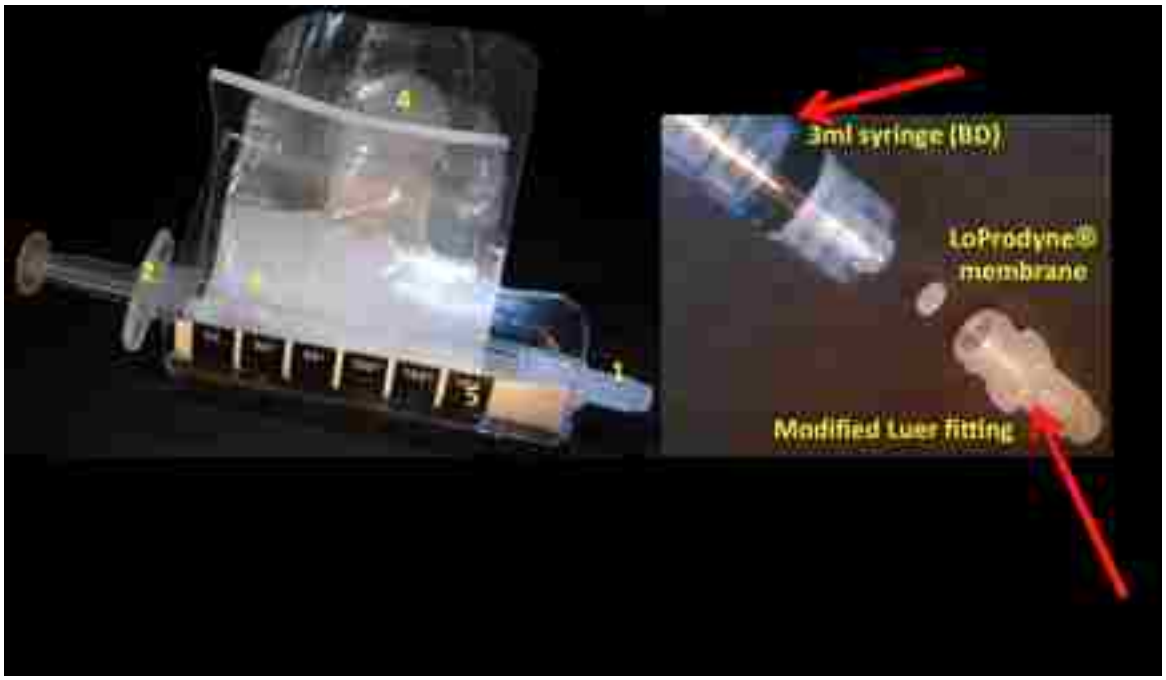

Figure 21. Initial prototype device design was used to develop and characterize assay system. This device configuration was designed for multiple usages.

Note: Prototype device design courtesy of LSDF Smart Card Project: Paul LaBarre, Shawn McGuire & Jered Singleton. Images adapted and modified from PATH and Professor James Lai.

The chemical (latent) heat is initiated by compressing the metallic button that produces an initial nucleation site for conversion of supersaturated sodium acetate liquid to a more

stable crystalline state. These pouches were designed for multiple usages through dissolution of crystallized sodium acetate in a heated water bath. **(5)** A thermoformed acrylic pouch housing was developed to provide additional insulation for the chemical heater as well as a liquid crystal thermometer visual indicator of "heater ready" status. This over housing holding the entire device **(3 &5)** was designed for multiple usages as well.

The complete self-powered prototype device was assembled as shown in **Figure 21.** Device performance was tested by measuring the variation of temperature with time of 1ml of 20% plasma solution within the prototype device.

Functional temperature range	38 ± 5°C
Ambient temperature range	20-25°C
Ramp to functional temperature	5 minutes maximum
Duration at functional temp range	15-30 minutes minimum
Sample volume	1-2 ml
Sample content	Plasma, DI water, PBS mix (optimize dilution)
Sample reservoir geometry	Basic BD 3ml plastic syringe (e.g. P/N 309585).
Process constraints	Before heating, user must be able to insert syringe assembly into heater. During heat step, user must be able to access and depress the syringe plunger. After heating, user must be able to remove assembly.
Activation	Simple, single step preferred

Table 5. Conceptual Specification of the prototype chemical heater developed for p24 assay (Courtesy of LSDF Smart Card Project)

3.3.2 Heating module using Phase Change Materials (PCMs)

The heating source was made up of a Scotchpak plastic film (Cat # PF450 CD) purchased from 3M. The optimized heating pack contains 20ml Phase Change Material (PCM) that is sodium acetate trihydrate in di-water (25% w/w) purchased from Sigma-Aldrich, Cat # 236500). The tip of the heating pack contains a concave stainless steel chip that will serve as a trigger for NAT crystallization. These chips were recycled from chemical heat pack purchased from Educational Innovations, Inc. (Part No. HEA-415). The ensemble device is held in a bent plastic mold, which we called broadband holder.

3.3.3. Non-Instrumented Syringe Device Performance Validation

The initial non-instrumented syringe flow-through device contained a syringe that incorporates a ca. 4 mm diameter membrane using a modified luer-lock adaptor as the membrane holder. The syringe was wrapped around with a heating component that contains phase change material heating pouch.

The optimal performance of this device requires specific characteristics similar to those described in **Table 4**. Here we tested the ability of the developed device to generate the required and sustained temperature for pNIPAAm LCST transition. The prototype heaters were tested using thermocouples and a digital thermometer. We used a digital thermocouple and an Infrared (IR) thermal camera to obtain the parameters for our assay development.

In the case of the digital thermocouple, we demonstrated that the prototype device maintained a temperature between 32°C-44°C degrees by measuring the temperatures of a few prototype devices with standard deviations. Briefly, we prepared a 1ml solution of

20% human plasma. This solution contained Streptavidin gold (40nm) conjugate, temperature responsive polymer-antibody conjugate 500mM NaCl and biotinylated antibody. Using a thermocouple, we recorded the temperatures of the 1ml samples every minute for four minutes. We plotted the variation of the temperatures with time to determine the sensitivity of the solution temperature within device vs. time.

In the case of an Infrared (IR) thermal camera our goal was to confirm that the given percentage of sodium acetate trihydrate required would yield the required heat levels when incorporated within plastic holder in the device. The final temperature of the sample inside the syringe embedded within the pouches would retain a constant temperature throughout the assay period. Here, black paint (Krylon, black) was used to reduce reflection and prevent interference of light on pouches surfaces. The IR images were collected using a FTIR camera (IR camara model XC6555) containing EXaminIR Max software. We obtain sodium acetate trihydrate crystallization video for 25% pouches.

3.3.3.1 pNIPAAm Mediated Surface Capture within Device using Membrane Holder

In order to demonstrate pNIPAAm-mediated capture mechanism of immunocomplexes during flow-through immunoassay within prototype device, we used salt (NaCl) together with temperature to induce aggregation of biotinylated pNIPAAm and Streptavidin gold nanoparticles. The objective of this experiment was to determine if there was a concentration dependent on the capture of AnNPs by the membrane within device at a fixed concentration of biotinylated pNIPAAm (bpNIPAAm, 13.3μM). The 40nm streptavidin colloidal gold conjugate used in this assay was purchased from Arista Biological Inc

(Product # CGSTV-0600) and was prepared from citrate coded gold through absorption of Streptavidin followed by passation using BSA.

We prepared samples with constant bpNIPAAm (15,000g/mol) concentrations in the 20% plasma and variable concentrations of SA-AuNPs in the 20% plasma. (Final concentrations: 0 .455μM, .909μM, 1.818μM and 3.636μM). The final volume of sample was 400ul. Prior to temperature initiation and flow-through, 500mM NaCl was added to each sample and pulled into the 3ml BD syringe using a needle. After assembling the device (**Figure 21**), the metallic clique on the heating pouch was triggered and sample moved across membrane after 5 minutes. Membranes were removed and scanned at 2400ppi to determine the MPI of the green channels.

3.3.3.2 pNIPAAm-antibody Mediated Capture of Partial Immunocomplex within Device

We wanted to confirm the specific capture of the half-sandwich immunocomplex in 20% human plasma samples on membrane filter within device. We demonstrated this by spiking different concentrations of p24 antigen in human plasma and subjecting the samples to different amounts of pNIPAAm-antibody conjugates (1-2000 molar excess). We used an anti-human CD4 pNIPAAm antibody conjugate as a negative control to evaluate the specificity of the system. Triplicate samples containing 100pg/ml p24 antigen to be tested were prepared in 20% human plasma for a variable range of anti-p24 polymer antibody conjugates. After the binding reaction, the tested samples were flown across membrane within device according to protocol outlined below with the exception of membrane quantification. Instead, flow-through samples were collected and tested for p24 antigen

content according to the PerkinElmer Life Sciences' HIV-1 p24 ELISA kit protocol outline above in **Chapter 2**.

3.3.3.3 Gold-labeled Flow-Though Immunoassay using this Prototype Device

3.3.3.3.1 Preparation of Biotinylated Anti-p24 mAb

The gold detection reagent system used employed Streptavidin biotin reagent system. Initially, we prepared biotinylated anti-p24 antibody using NHS-biotin labeling kits (Cat # 21335, Piece Biotechnology) following manufacturer's protocol. Biotinylated anti-p24 antibody samples were purified using desalting columns and degree of biotinylation was determined using HABA (4'-hydroxyazobenzene-2-carboxylic acid) assay. In that assay HABA, which is a weakly binding biotin analog, is bound to avidin, which alters its strong visible absorption at 500nm. Upon the addition of biotinylated antibody, the weaker binding HABA is displaced. We validated their activity using p24 antigen in house ELISA as described above (data not shown).

3.3.3.3.2 Assay principle: The flow-through assay is designed to quantitatively detect p24 antigen in human plasma matrix. When pNIPAAm-antibody conjugate and biotinylated antibody pairs are added to the p24 antigen in human plasma, they bind to complementary epitopes of the p24 antigen to form a sandwich immunocomplex. Upon addition of the Streptavidin gold nanoparticles, there is binding to form a thermally responsive gold sandwich immunocomplex. After incubation and heating within device, the sample is pushed across the embedded membrane filter via transverse capillarity and the aggregated complex is captured on the membrane filter.

All unbound reagents flow-through across the membrane. The assay is designed such that

the amount of captured immunocomplexes on the membrane surface would likely be proportional to the amount of p24 antigen spiked into human plasma solution hence, providing a semi-quantitative test. Because the concentration of HIV p24 antigen HIV found in patient plasma samples can be as low as a few picograms per milliliter, a larger volume sample gives the system an advantage of enrichment of total available biomarker to improve assay sensitivity. The assay is designed to detect picograms per milliliter p24 antigen. The native antigen used was standardized using PerkinElmer ELISA.

In order to quantify the amount of p24 antigen detected with the test samples we used image analysis (Image J) to obtain pixel intensities of the green channels of a membrane test spot (Region –of-interest (ROI)) relative to a control spot. This approach has been reported to quantify captured gold nanoparticles quantitatively on membrane surfaces[69].

3.3.3.3.3 Assay protocol: We prepared stock samples of all reagents and validated their concentrations appropriately using standard methods. For native p24 antigen stock (Cat # Cat # 14-101-050, Advanced Biotechnologies, Inc.), we used the FDA approved PerkinElmer ELISA kit to standardize all samples concentrations. The native p24 antigen was spiked into 100% fresh-pooled human plasma prepared using sodium EDTA (Valley Biomedical, Cat # HP 1052P). The final ratio of p24: conjugate: biotinylated antibody: Streptavidin-gold was 1: 18000:13500:135000 for 100 pg/ml p24. Initially, we moved 200ul of the spiked sample of known concentration of p24 antigen solution to a 1.5ml Eppendorf tube. We added all assay reagents and dilution buffer to a complete volume to 1ml (20% plasma). We then vortex sampled for 1 min and incubated for ~15 minutes at room temperature to form sandwich immune complexes. Before loading sample into

syringe, we added 500mM concentrated solution of NaCl to initiate aggregation. The 1ml sample solution was then transferred into the 3ml syringe using a needle. We then assembled the prototype device together with the loaded syringe as described in **Figure 21** above. After 3mins, we moved sample across membrane using the syringe plunger. The flow-through process took an average of 3-5 minutes, which amounted to an average manual flow rate of 200µl/min. At the end of the flow-through process, we removed the membrane from luer fittings and imaged them at a resolution of 2400 ppi using a Microtek ScanMaker i800 equipped with a CCD array tracks along the length of the scanner to make the image. The green channel image was cropped to circular field-of-view including the captured gold nanoparticles spots excluding the surrounding area and the ROI used for semi-quantification analysis.

Images were imported into image J and quantified by splitting into individual color channels and inverted to measure the mean pixel intensity (MPI) of green channel specific regions of the image. We compared MPI of blank membrane (background) to MPI of p24 antigen samples spiked into human plasma.

3.3.3.4 Assay Specificity and selectivity to individualized plasma samples

In this study, we tested our assay for false positive results generation using the assay protocol described above. We used a panel of 8 individual p24 negative human plasma specimens that were prepared from whole blood specimens using K-EDTA or Na-EDTA. Our collaborators at PATH provided these individualized human plasma samples.

3.3.3.5 Statistical evaluation

For all experiments, we collected data for triplicate samples and used them to calculate an

average. The averages were used to verify that the results obtained truly represent our concentration of samples or antigen tested. The collection of at least 3 data points allowed us to calculate the standard deviation. The standard deviation was used to measure how precisely the individual results agreed with each other.

4. Results and Discussion

4.1 Non-Instrumented syringe device performance validation

The fitting of the membrane holder was evaluated for leakage by flowing diluted spiked human plasma samples and was found to have a perfect fitting to syringe after modification of exterior. All the fabricated heating packs showed a consistent variation of temperature with time as indicated by the heating profile in **Figures 22 and 23** and IR images on **Figure 24**. There was minimal variation of temperature change with time amongst the individual heating packs. On an average, it took ~2.5-3minutes to reach peak temperatures of 39-41ºC which is the temperature required for flow-through immunoassay. This test confirms the required temperature that will trigger the polymer transition during immunoassays.

The performance of the prototype heater and device aligned with the specifications is outlined in **Table 5**. In summary, the prototype heaters tested with thermocouples as well as IR camera demonstrated required parameters needed for peak temperature (ca. 40°C) within 5 minutes and maintained above 32°C for more than 30 minutes. Therefore, we can conclude the prototype heater was sufficient to trigger the pNIPAAm-antibody conjugate aggregation during immunoassay.

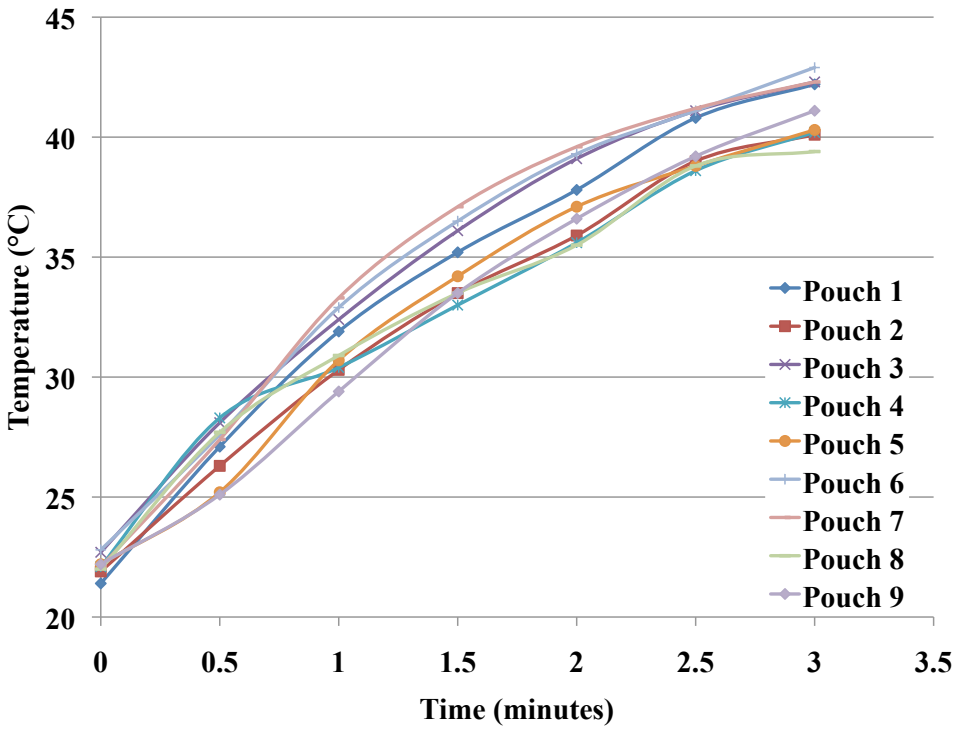

Figure 22. Heating profile of 9 individual heating packs within prototype device. The peak temperature of the solution inside the syringe was 40ºC within 3 minutes of initiation of phase change material aggregation.

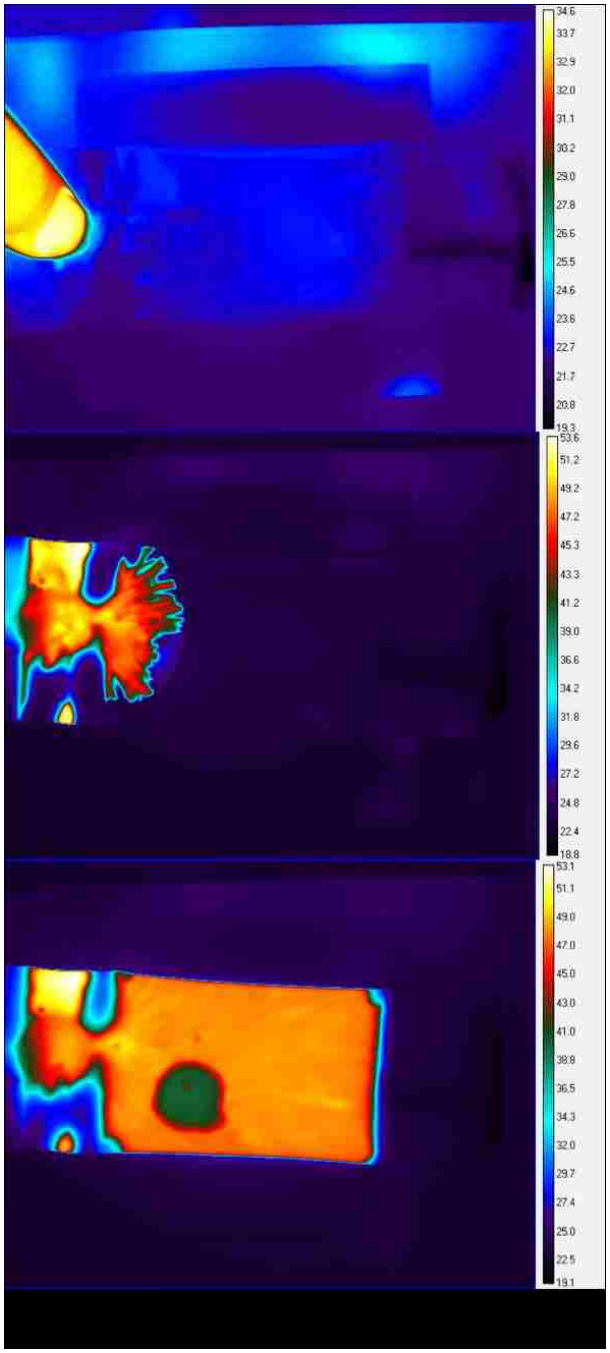

Figure 23. IR images of 20ml Sodium Acetate/ DI Water Mixture (25% wt/wt) in a heating pack showing high temperature of 43ºC

Note: This image was collected by the author, Shawn McGuire & Jered Singleton. Images adapted and modified from PATH.

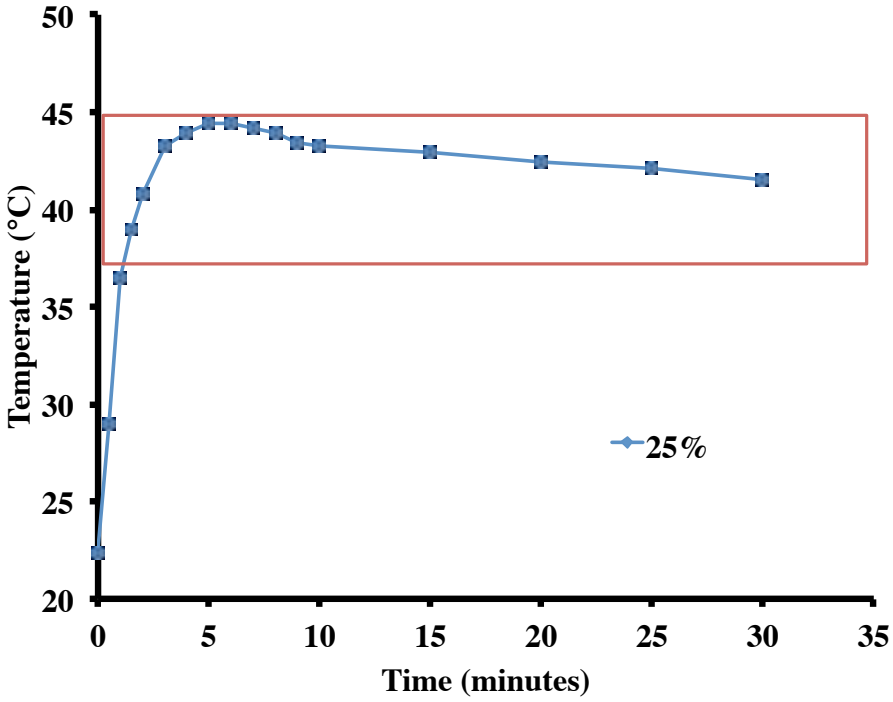

Figure 24. Heating profile of individual heating packs within prototype device showing temperature stability of exothermic reactions of sodium acetate trihydrate/water at 25% wt/wt. The peak temperature of the solution inside the syringe was measured within 30 minutes of initiation of phase change material aggregation. The peak temperature of the solution inside the syringe was 39 ± 4ºC within 3 minutes of initiation of phase change material aggregation. The red box indicates the required temperature regions.

A

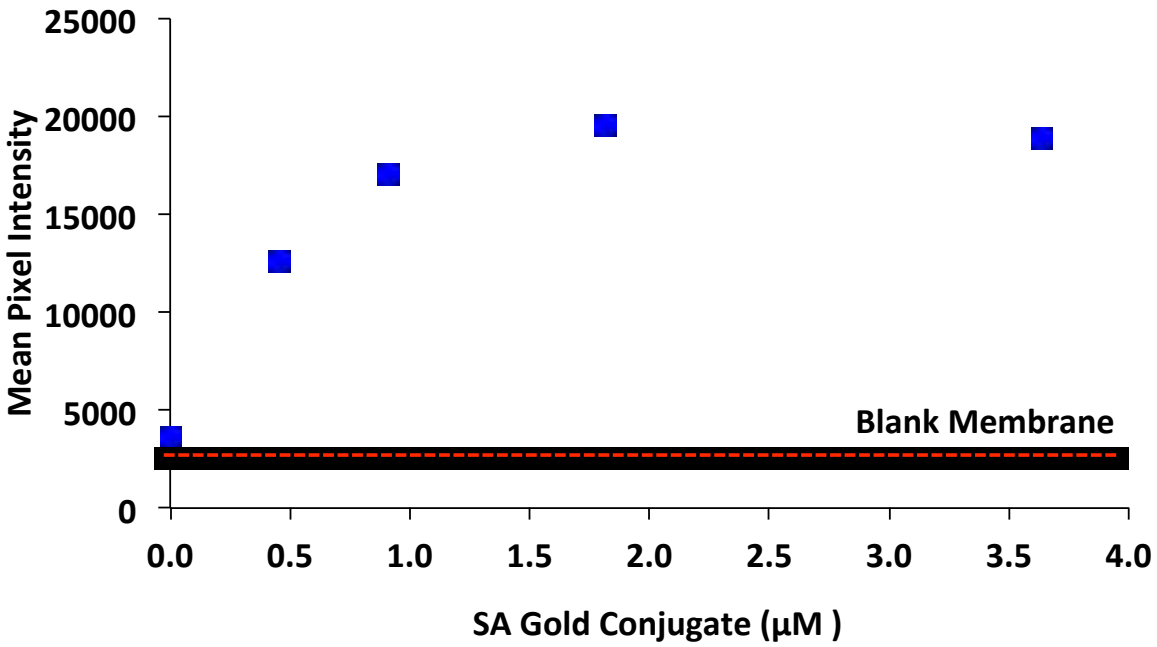

B

Figure 25. Capture of biotinylated pNIPAAm gold using prototype device A. Different concentrations of Sa-AuNPs was mixed with a fixed amount of bpNIPAAm, heated within device and flown across membrane. Membranes were then removed (A) and measured for amount of pNIPAAm-gold aggregates capture in mean pixel intensity. (B) Another control sample of SA-AuNPs without bpNIPAAm showed no capture.

3.4.2 Specific Capture of Polymer-antibody Conjugate and Bound p24 antigen on Membrane Filter within Device

We confirmed the specific capture of the half-sandwich immunocomplex in 20% human plasma samples on membrane filter within device upon phase transition of to pNIPAAm-antibody conjugates with bound p24 antigen. When the samples were heated, the p24 antigen half-sandwich immunocomplex formed aggregates with each other within syringe device. The flow-through mechanism of the syringe device is made possible due to the difference in atmospheric pressure and pressure generated within the syringe due to the movement of the syringe plunger. Aggregates were then captured by the membrane filter embedded within device **(Figure 21)** upon flow-through of samples. This is because the pNIPAAm upon heating above LCST residual interaction between the pNIPAAm side chain residue undergoes hydrophobic association between its hydrophobic groups in the pNIPAAm chains[70]. This phenomenon of pNIPAAm co-aggregation is transferred to pNIPAAm-antibody conjugates. Also, we have shown previously that the membrane filter (1.2 μm pore, nylon 6,6 membrane) can capture pNIPAAm aggregates upon interaction using the ELIFA (**Chapter 2**) system above.

The absorbance values for the positive control samples scaled with p24 antigen concentration were used to construct the standard curve. The negative control samples with anti-human CD4 polymer antibody conjugates showed absorbance values closer to the untreated samples indicating that the anti-human CD4 polymer conjugates did not bind p24 antigen non-specifically. This is because the binding epitopes of the anti-human CD4 polymer antibody conjugates are not complimentary to that of p24 antigen. For the test samples, we observed a decreasing OD for p24 antigen with increasing anti-p24 polymer

antibody conjugates concentration. Using standard curve and binding calculations explained above, we calculated the capture efficiency of p24 antigen at each polymer antibody conjugate amount as shown in **Figure 26.** We obtained ~77% capture efficiency for conjugate concentrations > 2000 molar excess which is very similar to our previous results and as seen previously by other binding studies.

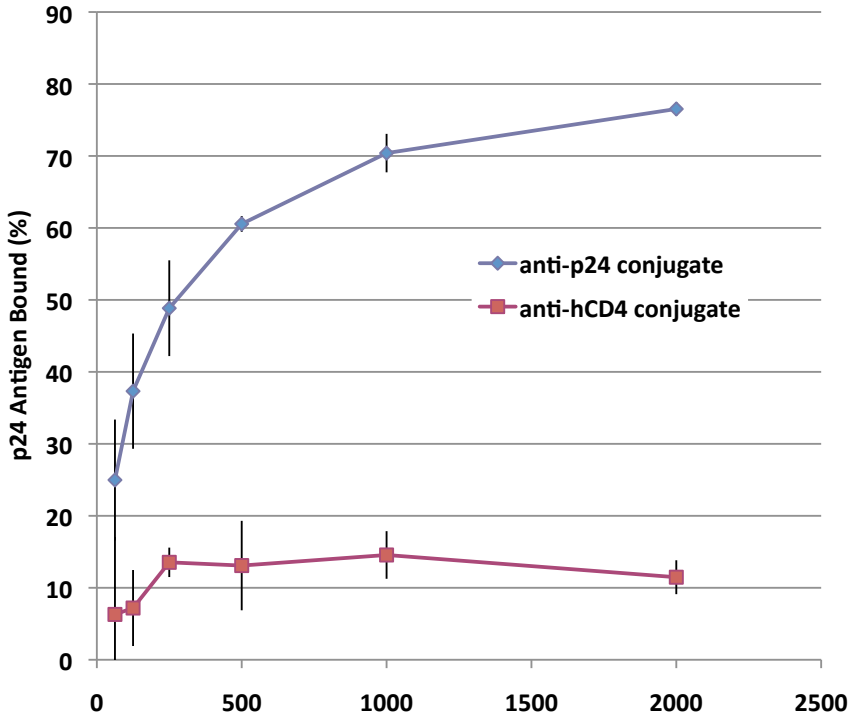

Figure 26. Specific capture of polymer–antibody conjugate with bound p24 antigen on membrane within device. p24 antigen samples (100pg/ml) in 20% plasma were treated with anti-hCD4 pNIPAAm conjugate and anti-p24 pNIPAAm conjugate and flown through filter (LoProdyne membrane). Binding reaction was performed at room temperature by incubating samples for 10 minutes followed by aggregates formation by pre-heating for 3 minutes at 40°C. The collected flow-through solutions were evaluated for p24 antigen content using PE kit p24 antigen ELISA. Results show that >75% p24 antigen was

recovered in the supernatant of the control sample treated anti-hCD4 pNIPAAm conjugate. Data represent mean of triplicates and error bars indicate standard deviation.

3.4.3 Preparation of Biotinylated Anti-p24 mAb

Successful biotinylation of detection anti-p24 antibodies was achieved by covalent conjugating to EZ-Link NHS-LC-LC-Biotin. This NHS-activated biotin reagent is known to react efficiently with primary amino groups ($-NH_2$) in the side chain of lysine (K) residues to form stable amide bonds in pH 7-9 buffers. After purification using a desalting column the degree of biotinylation was determined using the ratio of the absorbance at 500nm of avidin bound 2-(4-Hydroxyphenylazo) benzoic acid (HABA) with extinction coefficient $600M^{-1}cm^{-1}$ to the biotinylated antibody bound HABA with extinction coefficient 34500 $M^{-1}cm^{-1}$. This is because when avidin saturates HABA, the majority of the absorbance at 500 nm is due to bound HABA and the binding of biotinylated antibody displacing some or all of the HABA, hence a measurably lower absorbance. The measured ob absorbance ratio corresponded to 7-10 biotins per IgG.

3.4.4 Gold-labeled Flow-Though Immunoassay using this Prototype Device

In this experiment, we used gold in the place of enzyme to detect and quantify the enrichment of HIV-1 p24 assay using spiked human plasma specimens. We added all required reagents in the appropriate ratio with known amounts of diluted spiked human plasma specimens (0, 10, 20, 40 pg/ml) as final concentrations in 1ml samples. After 15 minutes of incubation the samples were pulled into the syringe using the plunger, wrapped

with heating pouch, placed inside prototype device holder and aggregation process initiated using the clicker on the heating pouch. Approximately 5 minutes later, samples were flown across membrane at the rate of 200ul/min. At the end of the flow-through process, the membranes were removed and acquired using a flatbed scanner for analysis.

Figure 27 shows the results of scanned membrane images and mean pixel intensity of the green channels of specific regions of interest (spots) of tested and control samples. The dash line indicates the background signal. There was a pink spot on the test samples compared to the control samples and the mean pixel intensities of the green channels for all test samples were greater than that of the control (membrane) as well as background (0pg/ml p24 antigen. Based on these results, these specimens tested positive for p24 antigen. We were able to detect 10pg/ml of p24 antigen in spiked human plasma specimens using gold-labeled flow-though immunoassay using this prototype device.

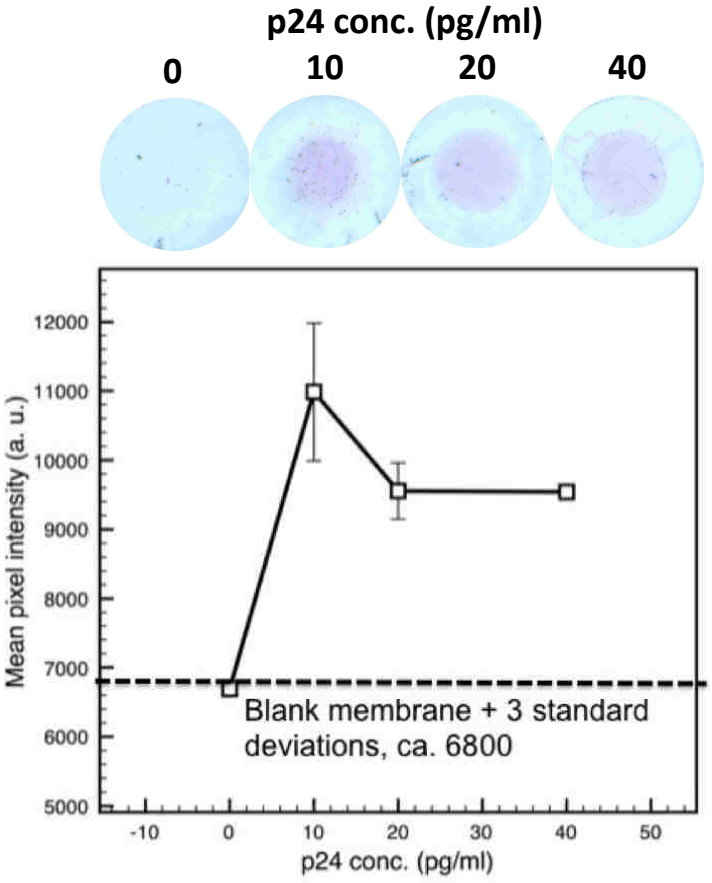

Figure 27. Pooled human plasma specimens with 20% dilutions giving final concentrations of 10-pg/ml p24. To perform the assays; we mixed stoichiometric reagent amounts as described in the protocol above. After 15 minutes incubation at room temperature, the solution was loaded into the syringe device, heated and flown across membrane filter. After flow-through, the membrane was removed and imaged using flatbed scanner. The dash line is the background signal, mean pixel intensity for the blank membrane plus 3 standard deviations. As seen by the background signal, the specimens in 20% human plasma with final concentrations of 10, 20 and 40-pg/mlp24 antigens were positive.

3.4.4 Assay Specificity and Selectivity to Individualized Plasma Samples

Figure 28 shows the results obtained from our assay specificity evaluation. Using the same reagent ratios and methods used in the assay development protocol, we determined the mean pixel intensity of each individual specimen tested including a blank membrane as a control.

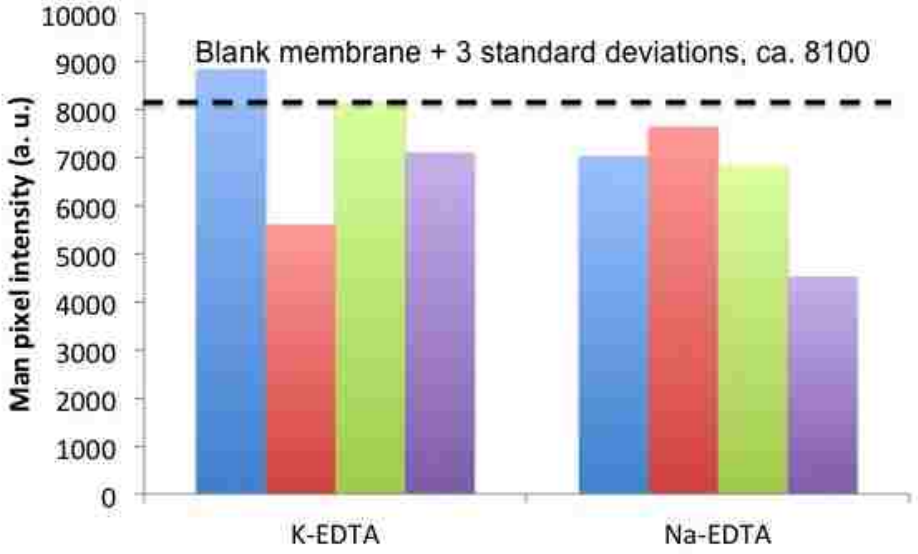

Figure 28. Assay specificity evaluation using negative human plasma specimen K-EDTA and Na-EDTA. Results showed 1 out of 8 individualized plasma samples tested false positive.

According to our background signal (control line ~ 8100, mean pixel intensity for the blank membrane plus 3 standard deviations) one out of the four K-EDTA human plasma showed false positive result. However, the assay signals for all four Na-EDTA specimens were all below the background. Based on these results, we were able to conclude that using Na-EDTA human plasma specimens for our assay development would lead to lower false positive rate. All assay optimization and dose response evaluation was performed using Na-EDTA human plasma specimens.

3.5. Conclusion

Here, we have outlined the successful identification of all the operating parameters, reagent ratios for the assay system by demonstrating assay sensitivity and specificity. We showed that low-level concentrations of samples could be tested for p24 antigen biomarker using our prototype non-instrumented device with to 10pg/ml sensitivity and the absences of false positive signal generation.

Chapter 4

Optimization of Non-instrumented Syringe Device with Gold-labeled Flow-through Assay

4.1 Introduction and Overview

In this chapter we optimize the flow-through rapid test (device and assay) to obtain a dose response. A dose–response relationship is important for our test development because during HIV infection, the levels of p24 antigen vary from patient to patient. By demonstrating a dose–response relationship we will have proven that our test is capable of identifying and distinguishing positive and negative HIV status among a wide range of HIV patients.

4.2 Experimental Design

The objective of the chapter was to investigate optimal conditions for the flow-through assay that would improve its performance to a dose response characterized by a curve of p24 dose response curve vs. p24 concentration with a correlation R >.90. Here, the previously Broadband prototype device was redesigned into a 3D clamshell plastic holder to improve stability and function and to provide more consistent heating (e.g., peak temperature, heating time).

We optimized reagent ratios by further characterization of SA-AUNPs. Finally, we varied the assay reagent ratios to enhance reproducibility of the assay system. We designed the experiment below based on standards approaches recommended by International Organization for Standardization Protocol ISO 8402:1994, the Laboratory Standards Institute (CLSI) Protocol EP17-A and report by Ambusher et al[71]. Experiments were

designed to determine the Limits of detection, Assay working range, Reproducibility and Precision and accuracy (Intra- and inter-assay coefficient of variation). For this method, we used the simplified definition of LOD according to the 1975 International Union of Pure and Applied Chemistry (IUPAC) which states that LOD is "A number expressed in units of concentration (or amount) that describes the lowest concentration level (or amount) of the element that an analyst can determine to be statistically different from an analytical blank"[72].

We followed previously reported method by Workman et al with slight modification[73]. The assay protocol we used is outlined below.

4.3 Materials and Methods

4.3.1 Clamshell Prototype Device or Smart Card Rapid Test Device

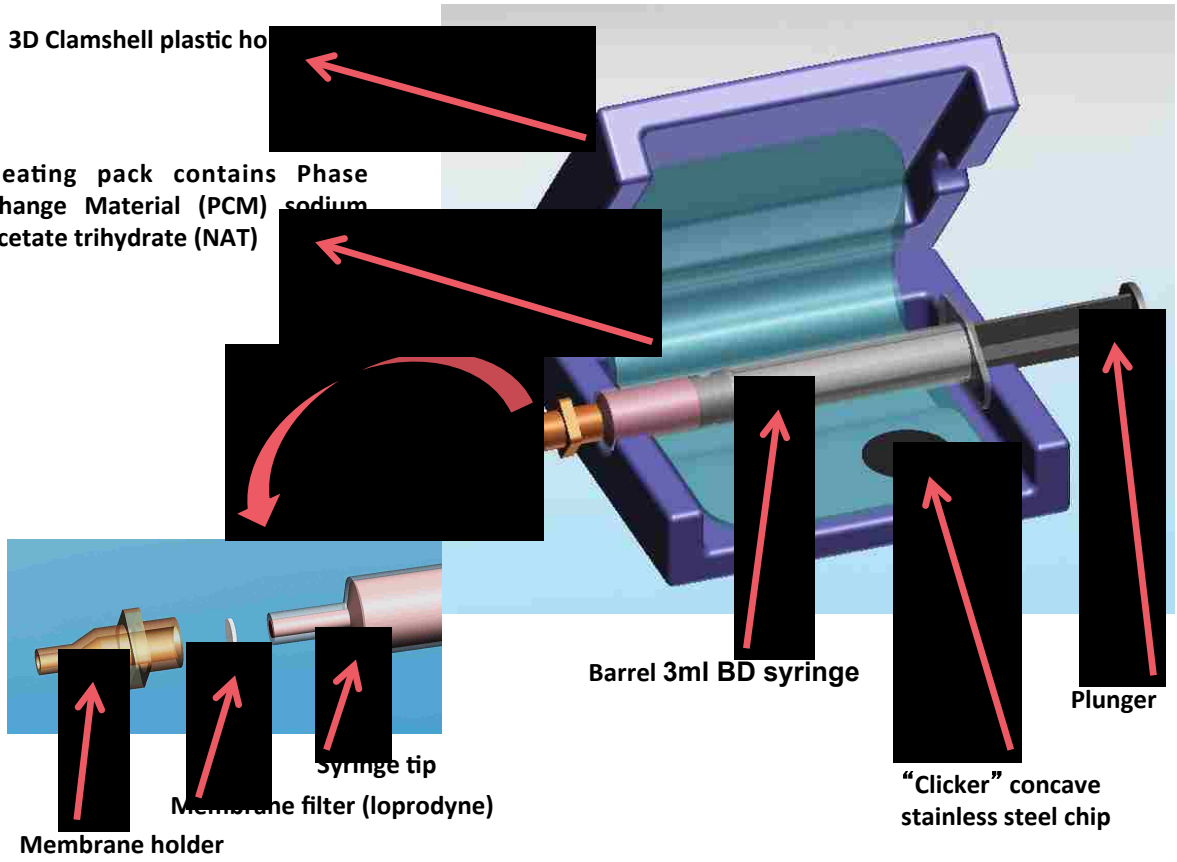

Figure 29. Annotated Clamshell prototype device. This image of self-powered prototype device was designed using Solidworks software.

Note: Prototype device design courtesy of LSDF Smart Card Project: Paul LaBarre, Shawn McGuire & Jered Singleton. Images adapted and modified from PATH and Professor James Lai.

The Clamshell prototype device was similar to the one described in **Chapter 3** with the exception of plastic holder. Here, a 3D Clamshell plastic holder was developed as an

improved design with better strength to enhance device performance. The complete self-powered prototype device was assembled as shown in **Figure 29**. Device performance was tested by measuring the variation of temperature with time of 1ml of 20% plasma solution within the prototype device as described in **Chapter 3**.

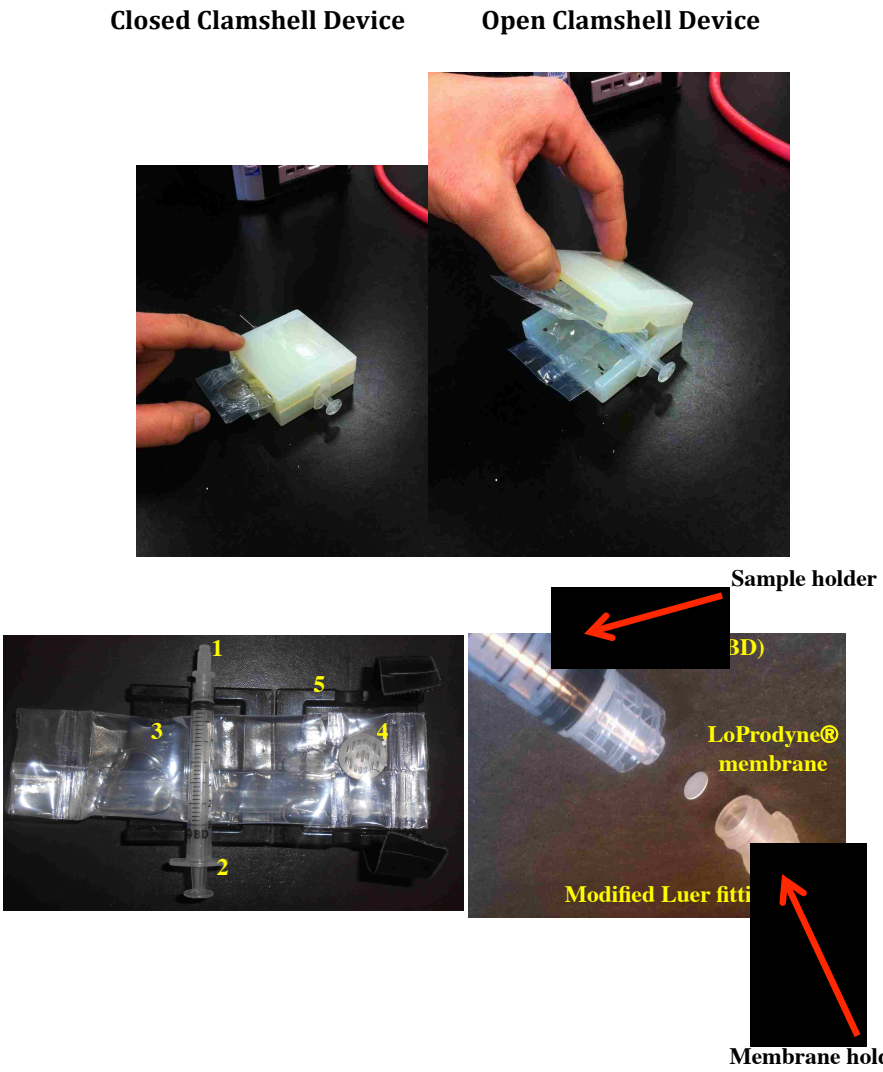

Note: Prototype device design courtesy of LSDF Smart Card Project: Paul LaBarre, Shawn McGuire & Jered Singleton. Images adapted and modified from PATH and Professor James Lai.

Figure 30. Prototype Self-Powered Device for Rapid HIV (p24 Antigen) Assay. (Top) Prototype device assembled before and after flow-through immunoassay. **(Bottom)** 1.

Modified Luer-lock with membrane filter 2. BD 3ml syringe 3. Heating pack-containing NAT in di-water (25% w/w) 4. Concave stainless steel chip 5. Clamshell plastic holder. The membrane filter (LoProdyne) was inserted into a modified luer-lock fitting as a membrane holder before device assembly. The membrane then captures the p24 sandwich immunocomplexes during the flow-through step after incubation and heating.

4.3.2 Binding sites of Gold Nanoparticles

Preparation of Gold Nanoparticle Antibody Conjugate

Similarly, the gold detection reagent system used the Streptavidin biotin reagent system. The biotinylated anti-p24 antibody was prepared a described in **Chapter 3**.

The 40nm Streptavidin colloidal gold conjugate used in this assay was purchased from Arista Biological Inc (Product # CGSTV-0600) and was prepared from citrate coded gold through absorption of Streptavidin followed by passation using BSA. Initially, we determined the amount of binding sides for Streptavidin gold conjugates in solution using the ability of biotin-4-fluorescein (B4F) Fisher Scientific Co LLC, (Cat # 50849911) fluorescence quenching by Streptavidin in terms of the B4F binding sites per ul of Streptavidin gold conjugates with fixed OD. Secondly, we proceeded to determine the effective binding sites on the colloidal gold conjugate using biotinylated antibodies. Briefly, to a 1.5ml Eppendorf tube, a mixture of Streptavidin gold conjugate (final OD = 0.2) and biotinylated antibodies (final concentration of 1-25nM) was incubated for 30 minutes at room temperature. All samples were in phosphate buffer saline, pH 7.4 containing 0.1mg/ml BSA. After incubation, 100ul of each sample was added to triplicate wells. Next, 25nM of biotin-4-fluorescein in the same buffer was prepared and immediately added to

each well making a final concentration of 12.5nM. After 10 minutes incubation fluorescence was measured at an excitation wavelength of 485nm and an emission wavelength of 535nm using a Tecan Safire^2 microplate reader. We then tested a higher dilution using 10UM biotin in triplicate as a positive control for the SA-NPs as well as testing for specificity.

4.3.3 Dose Response Studies

4.3.3.1 Optimized Flow-Through Immunoassay using Smart Card HIV Rapid Test

The improved Clamshell prototype device (**Figure 30)** was used to validate and develop the optimized gold immunoassay protocol in 1ml samples. Similarly, we prepared stock samples of all reagents and validated their concentrations appropriately using standard protocols. The native p24 antigen stock was standardized using FDA approved PerkinElmer p24 antigen ELISA kit as described in **Chapter 2**. The native p24 antigen was spiked into 100% fresh plasma prepared using sodium EDTA. The final reagent ratios were optimized sequentially. The final ratio of p24: conjugate: biotinylated antibody was 1: 15000:10000 for 100 pg/ml p24. The final ratio for the detection system was biotinylated antibody: Streptavidin-gold 7:1 for every moles of biotin binding site on the Streptavidin-gold colloids. Initially, we moved 200ul of the spiked sample of known concentration of p24 antigen solution to a 1.5ml Eppendorf tube. We then added all assay reagents and dilution buffer to a complete volume to 1ml (20% plasma). We then vortex sampled for 1 min and incubated for ~15 minutes at room temperature to form sandwich immune complexes. Before loading sample into syringe, we added 500mM concentrated solution of NaCl to initiate aggregation. The 1ml sample solution was then transferred into the 3ml syringe using a needle. We then assembled the prototype device together with the loaded syringe

as described in **Figure 30**. After 3mins, we moved sample across membrane using the syringe plunger at a manual flow rate of 200ul/min. The flow-through process takes 3-5 minutes. At the end of the flow-through process, we removed the membrane from Luer fittings for imaging and quantification analysis.

4.3.3.2 Membrane Spot Image Acquisition and Analysis

At the end of the flow-through process, we removed the membrane from Luer fittings and imaged them at a resolution of 2400 dpi in 48-bit RGB mode using a Microtek ScanMaker i800 equipped with a CCD array. Resulting RGB images were then imported into Image J and split into individual color channels and inverted. The green channel image was cropped to circular field-of-view including the captured gold nanoparticles spots excluding the surrounding area to measure the mean pixel intensity (MPI) of green channel specific regions of the image. We then subtracted the MPI of blank membrane (background) to MPI of negative control samples and p24 antigen samples spiked into human plasma. Using this method, we were able to correlate the integrated green channel pixel intensity at the p24 antigen test spots from the flow membranes for gold immunocomplexes to the native biomarker concentration to generate a dose response curve. All samples were run in triplicates and plotted as mean (standard

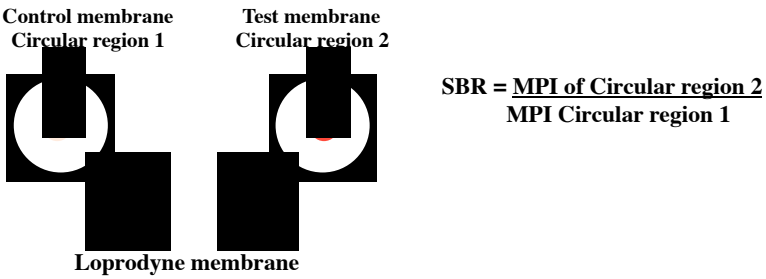

Figure 31. Illustration of membrane signal quantification approach using signal-to-background ratio (SBR).

deviation).

Quantitative analysis of the membrane signal was performed by calculation of the signal-to-background ratio of test spot with respect to control spot for all designated region-of-interest (ROI).

4.3.3.3 Statistical analysis

For all experiments, we collected data for triplicate samples and used them to calculate an average. The averages were used to verify that the results obtained truly represent our concentration of samples or antigen tested. The collection of at least 3 data points allowed us to calculate the standard deviation. The standard deviation was used to measure how precise the individual results agreed with each other. Using the analytical blank as a control, we performed statistical analysis on the working range of our assay system using student t-test.

4.4. Results and Discussion

4.4.1 Preparation of Gold Nanoparticle Antibody Conjugate

Successful biotinylation of detection anti-p24 antibodies was achieved by covalent conjugating to EZ-Link NHS-LC-LC-Biotin as previously discussed in **Chapter 3** yielding 7-10 biotins per IgG. We determined the effective binding sites per ul of Streptavidin gold conjugates with fixed OD in solution by biotinylated anti-p24 antibody using the ability of biotin-4-fluorescein fluorescence quenching by Streptavidin. We started by evaluating the quenching of SA-AuNPs solution (dilution 1: 50) with higher concentrations of biotinylated

antibodies and observed little or no quenching indicating that binding sites have been occupied until saturation. We then performed serial dilutions until we obtained a dynamic range. All experiments were performed in 1:1 dilution, 100ul B4F + 100ul SA-AuNP. We incubated 100ul of Streptavidin gold solution (OD=0.2) after binding interaction with biotinylated antibodies with 12.5nM biotin-4-fluorescein for 30mins. After 10 minutes incubation, fluorescence was measured at an excitation wavelength of 485 nm and an emission wavelength of 535 nm using a Tecan Safire^2 microplate reader. Fluorescence was measured at 485nm excitation (20nm bandwidth) and 535nm emission wavelength (20nm bandwidth).

The fluorescence of these wells was compared to that of 200 µl of the 12.5nM biotin-4-fluorescein solution measured at the same time. The relative fluorescence was calculated by dividing all fluorescence values by that of the positive control 12.5nM biotin-4-fluorescein. We then plotted the RFI values against the various biotinylated antibody concentrations. **Figure 32** shows the curve obtained from our results indicating that we observed a reduction in B4F quenching as we increased the amount of the biotinylated antibody until complete saturation of available binding sites on the gold surfaces in solution (point A on curve equals ~6.65nM) by the biotinylated antibody. Based on these results, we concluded that the 100ul Streptavidin gold solution (OD=0.2) has 6.65nM binding sites effectively occupied by biotinylated antibody. We optimized the assay format using a matched amount of biotin for each assay that yielded a maximum signal-to-background ratio.

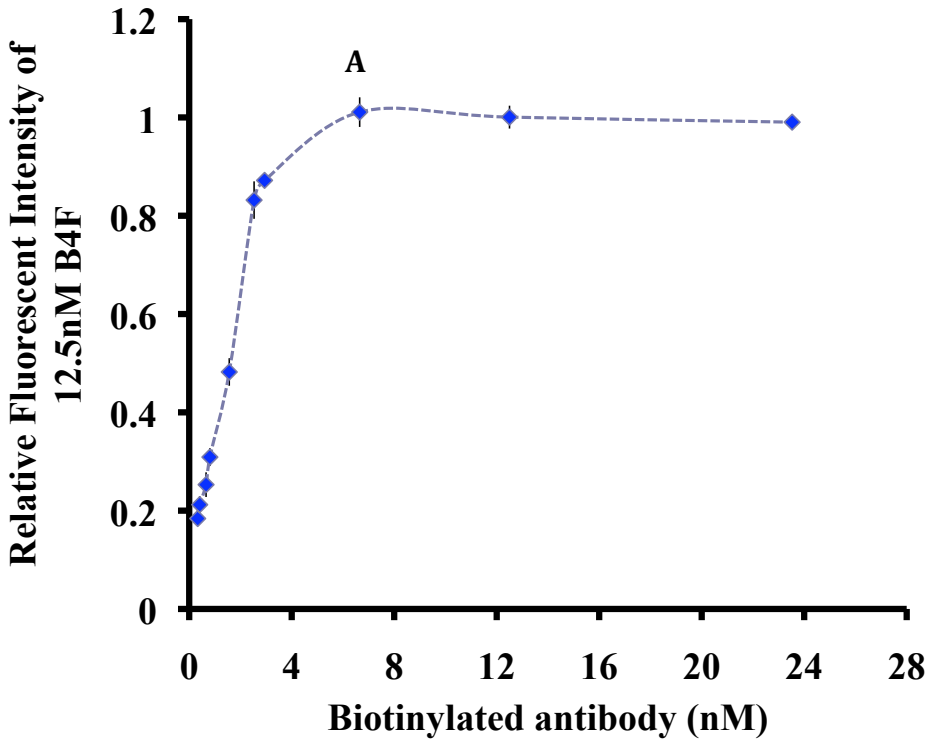

Figure 32. Effective binding sites determination of biotinylated antibody to a fixed amount of SA-AuNPs. The ability of biotin-4-fluorescien (B4F) fluorescence quenching by Streptavidin was used to estimate the number of binding sites available on SA-AuNPS. Samples were first mixed with different amounts of biotinylated antibody followed by a fixed amount of B4F. The incubation time was 30 minutes. The control sample was saturated with free biotin before incubation with analyte. The relative background-subtracted fluorescence was plotted as a function of different biotinylated antibody concentration. The figure shows the dependence of the fluorescence signal and the available number of binding sites on the nanoparticle. Data represent mean of triplicates and error bars indicate standard deviation.

4.4.2 Self-Powered Prototype Device Gold Flow-Through Immunoassay

The gold flow-through immunoassay was performed as described above. Pre-determined and optimized reagents (conjugates, p24 antigen-spiked plasma, detection antibodies and gold nanoparticles) were mixed together in an Eppendorf tube. After incubation for binding, samples were pulled into the syringe using the plunger. By pulling the syringe device, a partial vacuum was created inside the tube. The tip of the syringe needle exposed to immunocomplex sample where the pressure is higher than the inside of the tube of the syringe is pulled into the syringe by this higher pressure. After heating sample assembled within device as described in **Figure 30,** the sample is pushed across membrane filter slowing for 5 minutes.

The goal of the clamshell casing and PCM for heat generation was to improve reproducibility of heating device for the developed immunoassay module. The performance of the device was expected to match the parameters that were achieved using heating blocks or incubators or the broadband prototype device described in **Chapter 3**. The integrated system was then tested for its ability to reproduce results from previously developed assays (conjugates, p24 antigen-spiked plasma, detection antibodies and gold nanoparticles).

Finally, we performed several experiments to generate a dose response for p24 antigen rapid test. A dose–response relationship is essential to prove that our test is capable of identifying and distinguishing positive and negative HIV status among a wide range of HIV patients. Similar to assay formats above, p24 antigen in spiked human plasma was mixed with conjugates, detection antibodies and gold nanoparticles to form thermally responsive immunocomplexes. The samples were pulled by the plunger prior to device assembly and

allowed to heat within device to trigger aggregation. Upon flow-through the membrane then captures the gold-p24 sandwich immunocomplexes during the flow-through step after incubation and heating. The signal of the GNPs captured on the membrane surface should be proportional to the amount p24 present in the sample providing quantitative detection. We used established protocol to identify optimal reagent ratios necessary to generate a p24 antigen dose response. The main change here was the use of different reagent ratios and device optimization. We tested low-level concentrations of p24 antigen (12.5-

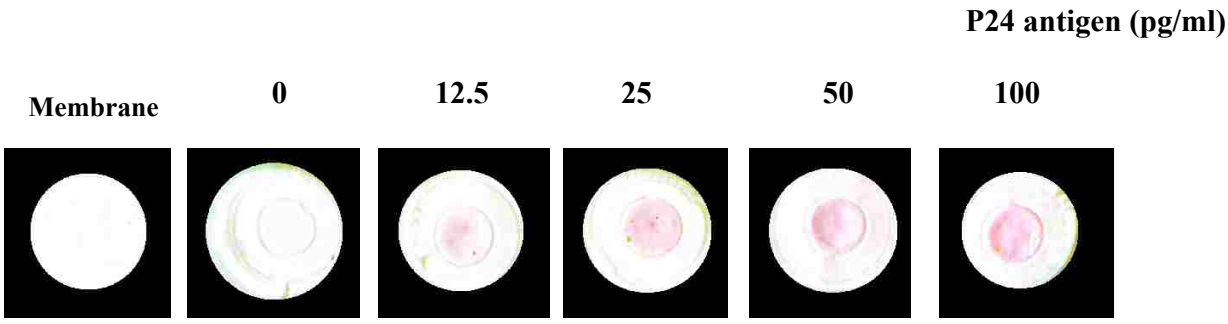

Figure 33. Performance of optimized flow-through immunoassay using Smart Card HIV Rapid Test. Scanned images of flow-though assay results experiments using 20% spike human plasma specimens (n=3). The resulting membrane images were taken using flatbed scanner set at a resolution of 2400ppi (Epson Expression 10000XL Flatbed color image scanner, which combines superior image processing by using a long-lasting Xenon lamp and Epson MatrixCCD technology).

100pg/ml) in human plasma samples. We collected measurements on different days, and the results for each sample set were scanned and analyzed to calculate the mean pixel intensity using Image J, signal-to-background ratio and coefficient of variation (COV) (%)

between samples and between runs. **Figure 33** shows the scanned membrane images of flow-through immunoassay used to detect p24 antigen in 20% spiked human plasma in three different experiments. The membranes samples did not contain target p24 antigen (negative controls or background), and did not show any signal. The samples containing 12.5-100pg/ml showed visible signals indicative of captured gold immunocomplexes. We developed and optimized an analytical method for quantification of our immunoassay results. In this method, scanned blank membrane MPI was subtracted from all individual values to obtain the background corrected MPIs. The respective MPIs were then used to calculate the signal-to-background ratio of each spot representing the Region of Interest (ROI), which was then plotted against p24 antigen concentration (data not shown). We observed a pink spot on the test samples compared to the control samples and the MPIs of the green channels for all test samples were greater than that of the control (membrane) as well as background (0pg/ml p24 antigen). As expected, the membrane signals were higher for all p24 antigen concentrations up until 100pg/ml above background signal (samples with no p24 antigen). Based on our result above, we can conclude that we have a semi-quantitative method for membrane image analysis using a background correction approach to eliminated noise, which causes imprecision in measurements of pixel intensity values. The data analysis method using background corrected MPI of scanned blank membrane appeared to be the best analytical method according to our results. We used this approach to further analyze our data.

Figure 34 shows the result obtained by testing 12 independent samples. The dash line indicates the control line with no p24 antigen present in the test samples (SBR = 1). This

line was used to differentiate levels of p24 antigen that can be detected by our immunoassay.

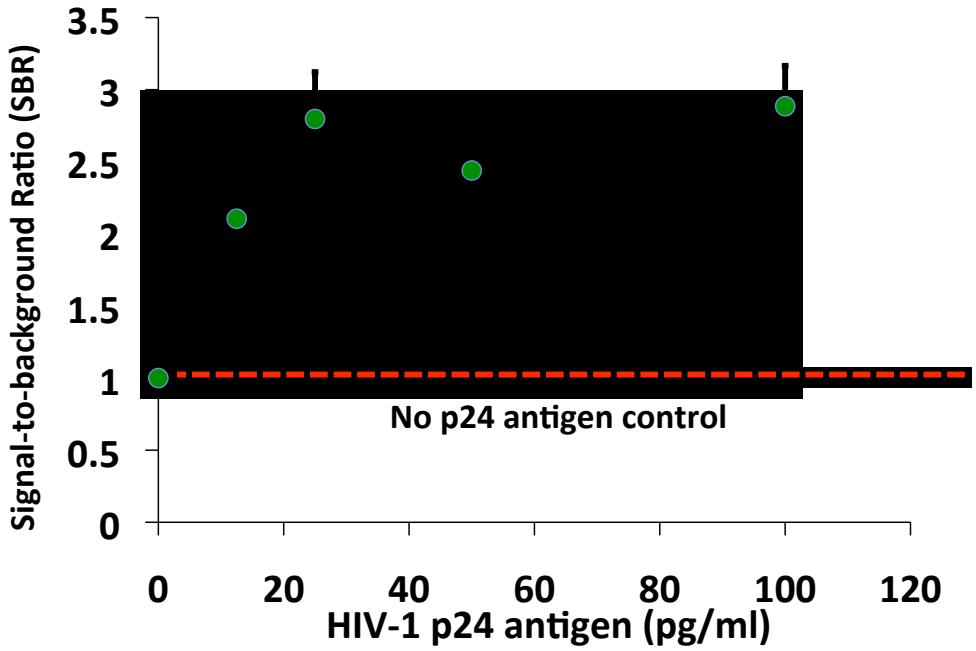

Figure 34. Data Analysis of optimized flow-through immunoassay using Smart Card HIV Rapid Test. The raw images were used to derive the mean pixel intensities (MPIs) from the same spot areas on both positive and negative sample. A blank membrane was used to subtract background signal generated by the membrane only before calculation of signal-to-background ratio for each sample. All tested HIV-1 p24 antigen samples (12.5 25, 50, and 100pg/ml) were all statistically significant in comparison to the analytical blank (0pg/ml) at using student t-test ($p<0.01$). Each data point represents the mean of 12 independent samples and error bar represents standard error.

As shown in **Figure 34**, all samples containing p24 antigen showed the higher SBR when compared with the control. This was also confirmed by statistical analysis using student t-test. The SBR for 12.5 25, 50, and 100 are all significantly higher in comparison to analytical blank or control (0) at $p<0.01$ by student t-test. Further testing showed that our assay was reproducible with COVs <15% as indicated by **Figure 35**.

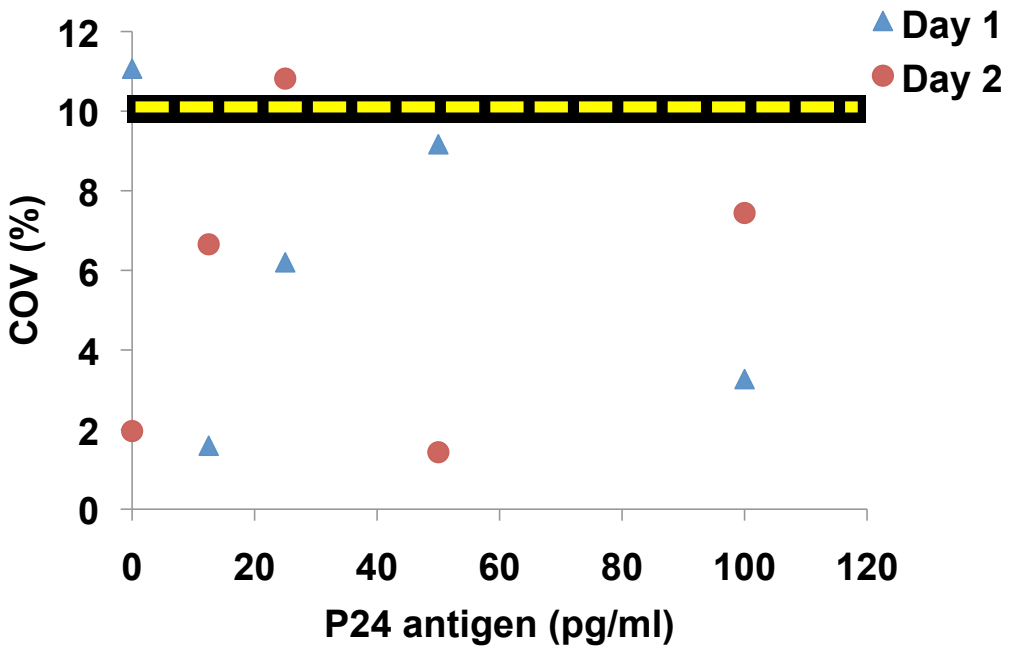

Figure 35. Smart Card HIV Rapid Test is Reproducible. Intra-run reproducibility of the p24 rapid assay for the detection of HIV-1 p24 antigen spiked into 20% plasma over triplicate runs of 3 individual samples on 2 different days.

In another analytic approach, we compared our Smart Card HIV Rapid Test to a gold standard. We used the assay results from our rapid test and compared the normalized signals with Reference EIA (**Figure 36**).

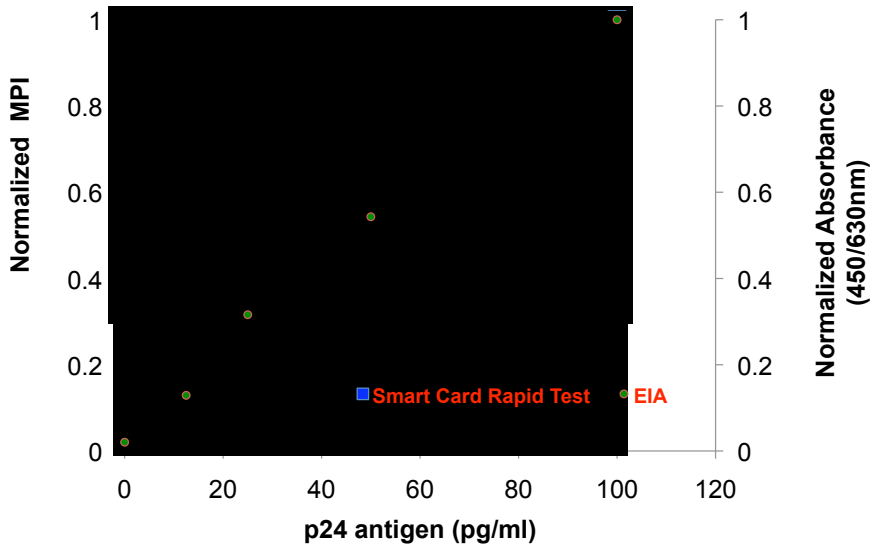

Figure 36. A comparison of a gold standard p24 antigen test (Enzyme Immunoassay (EIA) and Smart Card HIV Rapid Test. The normalized results of Smart Card HIV Rapid Test was compared to FDA approved p24 antigen ELISA as a Reference.

4.5 Conclusion

In this thesis, we have developed a flow-through immunoassay in plasma-spiked samples with the capture of the p24 immunocomplex on the membranes using enzyme conjugates capable of detecting 10pg/ml HIV-1 p24 antigen. We have also developed a flow-through immunoassay for plasma-spiked samples with capture of the p24 immunocomplex in a syringe device on the membranes using gold conjugates capable of detecting 12.5pg/ml HIV-1 p24 antigen. We have evaluated the assay performance in the syringe device using individual plasma spiked samples with different anti-coagulants (e.g., sodium citrate, heparin, EDTA). Specificity of the assay was evaluated using a panel of known HIV-negative specimens.

For the first time, pNIPAAm-antibody conjugate was used to develop a system that requires limited instrumentation, a very small amount of sample, and disposable device for detecting HIV-1 p24 antigen making the assay convenient for low resource settings. We present results showing the capture and detection of biomarker immunocomplexes enhanced by covalently modified IgG antibody-pNIPAAm conjugates and unmodified nylon-6, 6 membranes inserted within a flow-through device. The formation of a dual labeled immunocomplex sandwich in solution is specific and rapid at room temperature. The capture of immunocomplex aggregates is mediated by pNIPAAm above the LCST. Detection is mediated by subsequent antibody enzyme conjugate using a TMB precipitating substrate for disc device during initial phase of assay development and gold antibody conjugate during the final phase of assay development and device incorporation. We report experimental results demonstrating that this system provides rapid immunocomplex capture and detection for application to HIV-1 p24 antigen (12.5-100pg/ml) from spiked

human plasma samples, resulting in detection limits comparable to ELISA provided by centralized laboratories.

After series of assay optimization and device incorporation, we report the development of a low-cost immunoconcentration device for sensitive detection of HIV p24 antigen using our stimuli-responsive nanomaterial-based reagent technology and non-instrumented self-powered lab card devices format. For the first time, phase-separation immunoassay and phase-change materials were used to develop disposable devices employing limited instrumentation making assays convenient for LRSs. Our assay can accommodate a larger volume specimen (1ml) improving assay sensitivity by plasma p24 antigen (found in low concentrations) enrichment. We have demonstrated that the flow-through rapid assay systems have the potential to diagnose HIV-1 p24 antigen within clinically relevant concentrations similar to centralized lab tests.

In conclusion, we have used pNIPAAm-antibody conjugates to process large volumes (1ml) of HIV-1 p24 antigen plasma specimen through enrichment into concentration ranges that can be detected using flow-through visual detection systems in the presence of stimuli without instrumentation. These self-powered assays will be affordable, dependable and efficient for RLS with minimal usage training.

The clinical impact of HIV rapid testing technologies in patient care will be to achieve earlier, faster infection identification, allowing immediate counseling and treatment using ARVs.

Appendix A: Receptor-ligand Binding Theory for p24 antigen and Antibody

A. Mathematical Analysis and Simulations of p24 antigen Binding to Anti-p24 Antibody/Polymer-antibody Conjugates.

Ligand-receptor binding is an important biological problem. The mathematical treatment of binding reaction is based on the assumption that a single ligand binds to a single receptor in an independent reaction. The phenomenon is used to construct binding curves (Scatchard plots, Hill plots etc), which are one of the primary windows on the function of many molecules of biological interest. These calculations are made possible using the concept of chemical kinetics, equilibrium constant and the law of mass action to determine the dissociation constants of the ligand-receptor complex (Kd). Kd is interpreted as the ligand concentration at which the receptor has a probability of ½ being occupied. An immune complex formed from the integral binding of an antibody to a soluble antigen is a typical example of ligand-receptor binding.

Our goal is to find a simple model that predicts the fraction of receptors that have a ligand bound as a function of the ligand present. For this analysis p24 antigen=ligand (L) and antibody or smart conjugate=receptor(R) was used as a model. In order to obtain the theoretical antibody: p24 antigen ratios for optimal binding efficiency, we used a 1:1 antibody –antigen binding model (Ab + Ag ←→ Ab-Ag).

We construct binding curves at increasing amount of p24 antibody at constant p24 antigen concentrations (100pg/ml).

The stoichiometric equation of ligand-receptor binding from the point of view of equilibrium constants and the mass action is given by:

$$L + R \underset{Kd}{\overset{Ka}{\Leftrightarrow}} LR$$ ……L= Ligand, R= Receptor……**Equation 1**

		L	+	R	⇔	LR
	t=0	[L]		[R]		0
Equilibrium	t=∞	[L] - [RL]		[R] - [RL]		[RL]

$Ka = [RL]/ L] [R] \ldots M^{-1}$

Kd = [L] [R] / [RL] M……Law of Mass action……**Equation 2**

Ka = the association-dissociation constant

At equilibrium, equation 2 can be simplified into a quadratic equation as shown below:

$$Kd = [L] [R] / [RL]$$
$$= [L]- [RL] [R]-[RL]/ [RL]$$

$$[RL]^2 - [Kd + [L] + [R]] [RL] -[L] [R] = 0 \ldots\ldots\ldots\ldots\ldots\ldots\ldots\ldots\ldots\ldots\textbf{Equation 3}$$

a. Assumptions/Mass balance: Total ligand = Free ligand + Bound ligand

b. Percentage of occupied Ligand = [RL] / [L] + [LR]

Equation 3 can be solved using the quadratic formula of Mathematica software. Here, we used Mathematica software to generate binding curves for p24 antigen binding to anti-p24 antibody. All concentrations we converted in Pico molar.

B. The effect of increasing amount of p24 antibody at constant p24 antigen concentration (100pg/ml)

Using the binding concepts outlined above, the following binding curves were established.

The results of the curve above show that ~90% of p24 antigen is bound when antibody: p24 antigen ratio is 2048:1 (assuming that our antibody is performing at $Kd=10^{-9}M$).

The above ratio corresponds to ~8500pM of antibody or conjugate. Because we can obtain a high binding at this concentration, we used this concentration for our future simulations.

Here, we hypothesized that this concentration of antibody (8500pM) should bind with a similar or higher efficiency at p24 concentrations ≤100pg/ml.

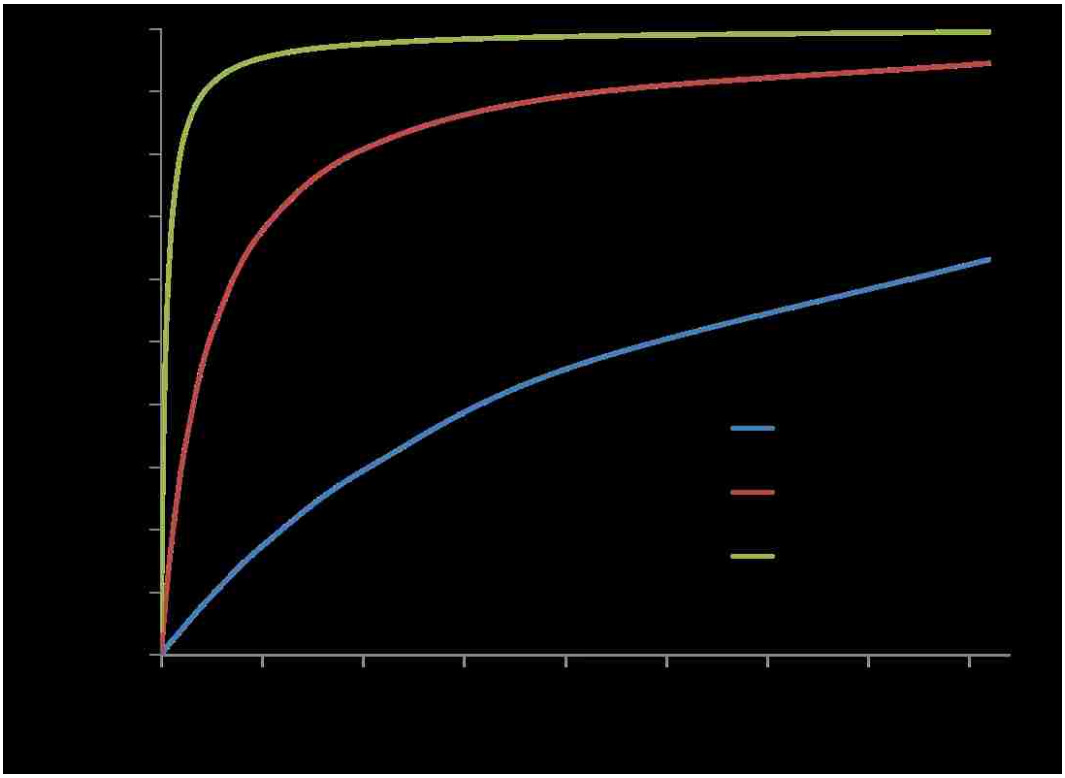

Figure 1. Binding simulations for 100pg/ml p24 antigen at various antibody: p24 antigen ratios.

Theoretical results and discussion

The summary table below shows the optimal binding efficiencies assuming Kd = 10^{-9}M at constant conjugate concentration (~8500pM).

P24 antigen (pg/ml)	Conjugate Molar Excess	% Bound p24 antigen
100 (4.18pM)	2048	~90
50 (2.09pM)	4096	~90
20 (0.84pM)	8192	~87
10 (0.42pM)	16384	~87

Based on this simulation results, we can conclude that a conjugate concentration of 8500pm can be used to bind > 80% p24 in solution. We used these results to perform our experiment.

BIBLIOGRAPHY

1. Koivunen, M. E.; Krogsrud, R. L., Principles of immunochemical techniques used in clinical laboratories. *Labmedicine* 2006, 37, (8).

2. Butto, S.; Suligoi, B.; Fanales-Belasio, E.; Raimondo, M., Laboratory diagnostics for HIV infection. *Annali Dell Istituto Superiore Di Sanita* 2010, 46, (1), 24-33.

3. Valkirs, G. E.; Barton, R., Immunoconcerntration - A new format for solid phase immunoassay. *Clinical Chemistry* 1985, 31, (9), 1427-1431.

4. Peeling, R. W.; Holmes, K. K.; Mabey, D.; Ronald, A., Rapid tests for sexually transmitted infections (STIs): the way forward. *Sexually Transmitted Infections* 2006, 82, V1-V6.

5. Kolosova, A. Y.; De Saeger, S.; Eremin, S. A.; Van Peteghem, C., Investigation of several parameters influencing signal generation in flow-through membrane-based enzyme immunoassay. *Analytical and Bioanalytical Chemistry* 2007, 387, (3), 1095-1104.

6. Posthuma-Trumpie, G. A.; Korf, J.; van Amerongen, A., Development of a competitive lateral flow immunoassay for progesterone: influence of coating conjugates and buffer components. *Analytical and Bioanalytical Chemistry* 2008, 392, (6), 1215-1223.

7. Andreotti, P. E.; Ludwig, G. V.; Peruski, A. H.; Tuite, J. J.; Morse, S. S.; Peruski, L. F., Immunoassay of infectious agents. *Biotechniques* 2003, 35, (4).

8. *UNAIDS World AIDS Day Report | 2011*.

9. Hall, H. I.; Song, R.; Rhodes, P.; Prejean, J.; An, Q.; Lee, L. M.; Karon, J.; Brookmeyer, R.; Kaplan, E. H.; McKenna, M. T.; Janssen, R. S.; Grp, H. I. V. I. S., Estimation of HIV incidence in the United States. *Jama-Journal of the American Medical Association* 2008, 300, (5), 520-529.

10. UNAIDS Report on the Global AIDS Epidemic. In Joint United Nations Programme on HIV/AIDS And World Health Organization, December 2012: 2012.

11. Marks, G.; Crepaz, N.; Janssen, R. S., Estimating sexual transmission of HIV from persons aware and unaware that they are infected with the virus in the USA. *Aids* 2006, 20, (10), 1447-1450.

12. Gurtler, L.; Muhlbacher, A.; Michl, U.; Hofmann, H.; Paggi, G. G.; Bossi, V.; Thorstensson, R.; Villaescusa, R. G.; Eiras, A.; Hernandez, J. M.; Melchior, W.; Donie, F.; Weber, B., Reduction of the diagnostic window with a new combined p24 antigen and human immunodeficiency virus antibody screening assay. *Journal of Virological Methods* 1998, 75, (1), 27-38.

13. Gurtler, L., Difficulties and strategies of HIV diagnosis. *Lancet* 1996, 348, (9021), 176-179.

14. Brennan, C. A.; Yamaguchi, J.; Vallari, A.; Swanson, P.; Hackett, J. R., ARCHITECT((R)) HIV Ag/Ab Combo assay: Correlation of HIV-1 p24 antigen sensitivity and RNA viral load using genetically diverse virus isolates. *Journal of Clinical Virology* 2013, 57, (2), 169-172.

15. Chavez, P.; Wesolowski, L.; Patel, P.; Delaney, K.; Owen, S. M., Evaluation of the performance of the Abbott ARCHITECT HIV Ag/Ab Combo Assay. *Journal of Clinical Virology* 2011, 52, S51-S55.

16. Weber, B.; Fall, E. H. M.; Berger, A.; Doerr, H. W., Reduction of diagnostic window by new fourth-generation human immunodeficiency virus screening assays. *Journal of Clinical Microbiology* 1998, 36, (8), 2235-2239.

17. Branson, B. M., State of the art for diagnosis of HIV infection. *Clinical Infectious Diseases* 2007, 45, S221-S225.

18. Malm, K.; von Sydow, M.; Andersson, S., Performance of three automated fourth-generation combined HIV antigen/antibody assays in large-scale screening of blood donors and clinical samples. *Transfusion Medicine* 2009, 19, (2), 78-88.

19. Saville, R. D.; Constantine, N. T.; Cleghorn, F. R.; Jack, N.; Bartholomew, C.; Edwards, J.; Gomez, P.; Blattner, W. A., Fourth-generation enzyme-linked immunosorbent assay for the simultaneous detection of human immunodeficiency virus antigen and antibody. *Journal of Clinical Microbiology* 2001, 39, (7), 2518-2524.

20. Wians, F. H.; Moore, H. A.; Briscoe, D.; Anderson, K. M.; Hicks, P. S.; Smith, D. L.; Clark, T. A.; Preton, M. M.; Gammons, B.; Ray, C. S.; Bond, C.; West, J. T., Evaluation of Four Qualitative Third-Generation HIV Antibody Assays and the Fourth-Generation Abbott HIV Ag/Ab Combo Test. *Labmedicine* 2011, 42, (9), 523-535.

21. Eshleman, S. H.; Khaki, L.; Laeyendecker, O.; Piwowar-Manning, E.; Johnson-Lewis, L.; Husnik, M.; Koblin, B.; Coates, T.; Chesney, M.; Vallari, A.; Devare, S. G.; Hackett, J., Detection of Individuals With Acute HIV-1 Infection Using the ARCHITECT HIV Ag/Ab Combo Assay. *Jaids-Journal of Acquired Immune Deficiency Syndromes* 2009, 52, (1), 121-124.

22. Suligoi, B.; Rodella, A.; Raimondo, M.; Regine, V.; Terlenghi, L.; Manca, N.; Casari, S.; Camoni, L.; Salfa, M. C.; Galli, C., Avidity Index for Anti-HIV Antibodies: Comparison between Third- and Fourth-Generation Automated Immunoassays. *Journal of Clinical Microbiology* 2011, 49, (7), 2610-2613.

23. Schupbach, J., Measurement of HIV-1 p24 antigen by signal-amplification-boosted ELISA of heat-denatured plasma is a simple and inexpensive alternative to tests for viral RNA. *AIDS Reviews* 2002, 4, (2), 83-92.

24. Taegtmeyer, M.; MacPherson, P.; Jones, K.; Hopkins, M.; Moorcroft, J.; Lalloo, D. G.; Chawla, A., Programmatic Evaluation of a Combined Antigen and Antibody Test for Rapid HIV Diagnosis in a Community and Sexual Health Clinic Screening Programme. *Plos One* 2011, 6, (11).

25. Pavie, J.; Rachline, A.; Loze, B.; Niedbalski, L.; Delaugerre, C.; Laforgerie, E.; Plantier, J.-C.; Rozenbaum, W.; Chevret, S.; Molina, J.-M.; Simon, F., Sensitivity of Five Rapid HIV Tests on Oral Fluid or Finger-Stick Whole Blood: A Real-Time Comparison in a Healthcare Setting. *Plos One* 2010, 5, (7).

26. Dinnes, J.; Deeks, J.; Kunst, H.; Gibson, A.; Cummins, E.; Waugh, N.; Drobniewski, F.; Lalvani, A., A systematic review of rapid diagnostic tests for the detection of tuberculosis infection. *Health Technology Assessment* 2007, 11, (3), 1-+.

27. Lee, H. H.; Dineva, M. A.; Chua, Y. L.; Ritchie, A. V.; Ushiro-Lumb, I.; Wisniewski, C. A., Simple Amplification-Based Assay: A Nucleic Acid Based Point-of-Care Platform for HIV-1 Testing. *Journal of Infectious Diseases* 2010, 201, S65-S72.

28. Tang, S.; Hewlett, I., Nanoparticle-Based Immunoassays for Sensitive and Early Detection of HIV-1 Capsid (p24) Antigen. *Journal of Infectious Diseases* 2010, 201, S59-S64.

29. Parpia, Z. A.; Elghanian, R.; Nabatiyan, A.; Hardie, D. R.; Kelso, D. M., p24 Antigen Rapid Test for Diagnosis of Acute Pediatric HIV Infection. *Jaids-Journal of Acquired Immune Deficiency Syndromes* 2010, 55, (4), 413-419.

30. Nabatiyan, A.; Baumann, M. A.; Parpia, Z.; Kelso, D., A Lateral Flow-Based Ultra-Sensitive p24 HIV Assay Utilizing Fluorescent Microparticles. *Jaids-Journal of Acquired Immune Deficiency Syndromes* 2010, 53, (1), 55-61.

31. Parpia, Z. A.; Elghanian, R.; Nabatiyan, A.; Hardie, D. R.; Kelso, D. M., p24 antigen rapid test for diagnosis of acute pediatric HIV infection. *J Acquir Immune Defic Syndr* 2010, 55, (4), 413-9.

32. Schito, M. L.; D'Souza, M. P.; Owen, S. M.; Busch, M. P., Challenges for Rapid Molecular HIV Diagnostics. *Journal of Infectious Diseases* 2010, 201, S1-S6.

33. Greer, L.; Wendel, G. D., Rapid Diagnostic Methods in Sexually Transmitted Infections. *Infectious Disease Clinics of North America* 2008, 22, (4), 601-+.

34. *KonstantinLyashchenk*o, *J. E. R. G. D. G.*, Rapid test for *TB/HIV co-infection. Chembio Diagnostic Systems, Inc., Medford, NY, USA*.

35. Malonza, I. A.; Richardson, B. A.; Kreiss, J. K.; Bwayo, J. J.; Stewart, G. C. J., The effect of rapid HIV-1 testing on uptake of perinatal HIV-1 interventions: a randomized clinical trial. *Aids* 2003, 17, (1), 113-118.

36. Busch, M. P.; Kleinman, S. H.; Nemo, G. J., Current and emerging infectious risks of blood transfusions. *Jama-Journal of the American Medical Association* 2003, 289, (8), 959-962.

37. Lindback, S.; Thorstensson, R.; Karlsson, A. C.; von Sydow, M.; Flamholc, L.; Blaxhult, A.; Sonnerborg, A.; Biberfeld, G.; Gaines, H.; Karolinska Inst Primary, H. I. V. I., Diagnosis of primary HIV-1 infection and duration of follow-up after HIV exposure. *Aids* 2000, 14, (15), 2333-2339.

38. LaBarre, P.; Hawkins, K. R.; Gerlach, J.; Wilmoth, J.; Beddoe, A.; Singleton, J.; Boyle, D.; Weigl, B., A Simple, Inexpensive Device for Nucleic Acid Amplification without Electricity-Toward Instrument-Free Molecular Diagnostics in Low-Resource Settings. *Plos One* 2011, 6, (5).

39. Heskins, M.; Guillet, J. E., Solution properties of poly(N-isopropylacrylamide). *Journal of Macromolecular Science, Chemistry* 1968, 2, (8), 1441-55.

40. Malmstadt, N.; Hyre, D. E.; Ding, Z.; Hoffman, A. S.; Stayton, P. S., Affinity thermoprecipitation and recovery of biotinylated biomolecules via a mutant streptavidin-smart polymer conjugate. *Bioconjug Chem* 2003, 14, (3), 575-80.

41. Malmstadt, N.; Yager, P.; Hoffman, A. S.; Stayton, P. S., A smart microfluidic affinity chromatography matrix composed of poly(N-isopropylacrylamide)-coated beads. *Anal Chem* 2003, 75, (13), 2943-9.

42. Kulkarni, S.; Schilli, C.; Muller, A. H.; Hoffman, A. S.; Stayton, P. S., Reversible meso-scale smart polymer--protein particles of controlled sizes. *Bioconjug Chem* 2004, 15, (4), 747-53.

43. Malmstadt, N.; Hoffman, A. S.; Stayton, P. S., "Smart" mobile affinity matrix for microfluidic immunoassays. *Lab Chip* 2004, 4, (4), 412-5.

44. Ebara, M.; Hoffman, J. M.; Hoffman, A. S.; Stayton, P. S., Switchable surface traps for injectable bead-based chromatography in PDMS microfluidic channels. *Lab Chip* 2006, 6, (7), 843-8.

45. Kulkarni, S.; Schilli, C.; Grin, B.; Muller, A. H.; Hoffman, A. S.; Stayton, P. S., Controlling the aggregation of conjugates of streptavidin with smart block copolymers prepared via the RAFT copolymerization technique. *Biomacromolecules* 2006, 7, (10), 2736-41.

46. Lai, J. J.; Hoffman, J. M.; Ebara, M.; Hoffman, A. S.; Estournes, C.; Wattiaux, A.; Stayton, P. S., Dual magnetic-/temperature-responsive nanoparticles for microfluidic separations and assays. *Langmuir* 2007, 23, (13), 7385-91.

47. Narain, R.; Gonzales, M.; Hoffman, A. S.; Stayton, P. S.; Krishnan, K. M., Synthesis of monodisperse biotinylated p(NIPAAm)-coated iron oxide magnetic nanoparticles and their bioconjugation to streptavidin. *Langmuir* 2007, 23, (11), 6299-304.

48. Lai, J. J.; Nelson, K. E.; Nash, M. A.; Hoffman, A. S.; Yager, P.; Stayton, P. S., Dynamic bioprocessing and microfluidic transport control with smart magnetic nanoparticles in laminar-flow devices. *Lab Chip* 2009, 9, (14), 1997-2002.

49. Golden, A. L.; Battrell, C. F.; Pennell, S.; Hoffman, A. S.; Lai, J. J.; Stayton, P. S., Simple fluidic system for purifying and concentrating diagnostic biomarkers using stimuli-responsive antibody conjugates and membranes. *Bioconjug Chem* 2010, 21, (10), 1820-6.

50. Hoffman, J. M.; Ebara, M.; Lai, J. J.; Hoffman, A. S.; Folch, A.; Stayton, P. S., A helical flow, circular microreactor for separating and enriching "smart" polymer-antibody capture reagents. *Lab Chip* 2010, 10, (22), 3130-8.

51. Nash, M. A.; Lai, J. J.; Hoffman, A. S.; Yager, P.; Stayton, P. S., "Smart" diblock copolymers as templates for magnetic-core gold-shell nanoparticle synthesis. *Nano Lett* 2010, 10, (1), 85-91.

52. Stayton, P. S.; Nash, M.; Lai, J., System and Method for Magnetically Concentrating and Detecting Biomarkers. In Google Patents: 2010.

53. Stayton, P. S.; Domingo-Villegas, G. J.; Golden, A.; Lai, J.; Nash, M. A.; Weigl, B. H.; Fomban, N. T. G.; Labarre, P., SELF-POWERED SMART DIAGNOSTIC DEVICES. In Google Patents: 2010.

54. Stayton, P. S.; Hoffman, A. S.; Lai, J.; Hoffman, J.; Ebara, M., Stimuli-responsive magnetic nanoparticles and related methods. In Google Patents: 2011.

55. Golden, A. L.; Battrell, C. F.; Pennell, S.; Hoffman, A. S.; Lai, J. J.; Stayton, P. S., Simple Fluidic System for Purifying and Concentrating Diagnostic Biomarkers Using Stimuli-Responsive Antibody Conjugates and Membranes. *Bioconjugate Chemistry* 2010, 21, (10), 1820-1826.

56. Malmstadt, N.; Hoffman, A. S.; Stayton, P. S., "Smart" mobile affinity matrix for microfluidic immunoassays. *Lab on a Chip* 2004, 4, (4), 412-415.

57. Hoffman, A. S.; Stayton, P. S.; Shimoboji, T.; Chen, G. H.; Ding, Z. L.; Chilkoti, A.; Long, C.; Miura, M.; Chen, J. P.; Park, T.; Monji, N.; Cole, C. A.; Harris, J. M.; Nakamae, K., Conjugates of stimuli-responsive polymers and biomolecules: Random and site-specific conjugates of temperature-sensitive polymers and proteins. *Macromolecular Symposia* 1997, 118, 553-563.

58. Hoffman, A. S.; Stayton, P. S.; Bulmus, V.; Chen, G. H.; Chen, J. P.; Cheung, C.; Chilkoti, A.; Ding, Z. L.; Dong, L. C.; Fong, R.; Lackey, C. A.; Long, C. J.; Miura, M.; Morris, J. E.; Murthy, N.; Nabeshima, Y.; Park, T. G.; Press, O. W.; Shimoboji, T.; Shoemaker, S.; Yang, H. J.; Monji, N.; Nowinski, R. C.; Cole, C. A.; Priest, J. H.; Harris, J. M.; Nakamae, K.; Nishino, T.; Miyata, T., Really smart bioconjugates of smart polymers and receptor proteins. *Journal of Biomedical Materials Research* 2000, 52, (4), 577-586.

59. Hoffman, A. S.; Stayton, P. S., Bioconjugates of smart polymers and proteins: Synthesis and applications. *Macromolecular Symposia* 2004, 207, 139-151.

60. Wu, J.; Fu, Z.; Yan, F.; Ju, H., Biomedical and clinical applications of immunoassays and immunosensors for tumor markers. *Trac-Trends in Analytical Chemistry* 2007, 26, (7), 679-688.

61. de la Escosura-Muniz, A.; Merkoci, A., A Nanochannel/Nanoparticle-Based Filtering and Sensing Platform for Direct Detection of a Cancer Biomarker in Blood. *Small* 2011, 7, (5), 675-682.

62. Jain, K. K., Applications of nanobiotechnology in clinical diagnostics. *Clinical Chemistry* 2007, 53, (11), 2002-2009.

63. Wilson, R., The use of gold nanoparticles in diagnostics and detection. *Chemical Society Reviews* 2008, 37, (9), 2028-2045.

64. Butler, J. E., *Solid phases in immunoassay*. 1996; p 205-225.

65. Neises, B.; Steglich, W., 4-dialkylaminopyridines as acylation catalysts. .5. Simple methods for esterification of carboxylic-acids. *Angewandte Chemie-International Edition in English* 1978, 17, (7), 522-524.

66. Salomi, B. S. B.; Mitra, C. K., Electrochemical studies on horseradish peroxidase covalently coupled with redox dyes. *Biosensors & Bioelectronics* 2007, 22, (8), 1825-1829.

67. Gazaryan, I. G.; Klyachko, N. L.; Dulkis, Y. K.; Ouporov, I. V.; Levashov, A. V., Formation and properties of dimeric recombinant horseradish peroxidase in a system of reversed micelles. *Biochemical Journal* 1997, 328, 643-647.

68. Voller, A.; Bidwell, D. E.; Bartlett, A., Enzyme immunoassays in diagnostic medicine-theory and practice. *Bulletin of the World Health Organization* 1976, 53, (1), 55-65.

69. Rohrman, B. A.; Leautaud, V.; Molyneux, E.; Richards-Kortum, R. R., A Lateral Flow Assay for Quantitative Detection of Amplified HIV-1 RNA. *Plos One* 2012, 7, (9).

70. Cho, E. C.; Lee, J.; Cho, K., Role of bound water and hydrophobic interaction in phase transition of poly(N-isopropylacrylamide) aqueous solution. *Macromolecules* 2003, 36, (26), 9929-9934.

71. Armbruster, D. A.; Tillman, M. D.; Hubbs, L. M., Limit of detection (LOD) Limit of quantification (LOQ) - comparison of the empirical and the statistical , methods exemplified with GC-MS assays of abused drugs. *Clinical Chemistry* 1994, 40, (7), 1233-1238.

72. Numenclature, symbols, units and their usage in spectrochemical analysis .2. Data interpretation. *Spectrochimica Acta Part B-Atomic Spectroscopy* 1978, 33, (6), 242-245.

73. Workman, S.; Wells, S. K.; Pau, C.-P.; Owen, S. M.; Dong, X. F.; LaBorde, R.; Granade, T. C., Rapid detection of HIV-1 p24 antigen using magnetic immuno-chromatography (MICT). *Journal of Virological Methods* 2009, 160, (1-2), 14-21.